Structures 58 (2023) 105474

Contents lists available at ScienceDirect

Structures

journal homepage: www.elsevier.com/locate/structures

A review on the shear performance of reinforced concrete (RC) beams strengthened with externally bonded mortar-based composites

Xiangsheng Liu [a,*], Georgia E. Thermou [b]

[a] Centre for Structural Engineering and Informatics, Dept. of Civil Engineering, The University of Nottingham, NG7 2RD Nottingham, UK
[b] Assistant Professor in Structural Engineering, Dept. of Civil Engineering, The University of Nottingham, NG7 2RD Nottingham, UK

ARTICLE INFO

Keywords:
Reinforced concrete
Beam
Mortar-based composites
Shear
Strengthening
Retrofitting
FRCM
FRC
ECC
UHPFRC

ABSTRACT

This paper reviews the performance of shear strengthened reinforced concrete (RC) beams with the use of externally bonded mortar-based composite jackets (e.g. FRCM, ECC, UHPFRC). An experimental database was compiled gathering all the known studies in strengthening shear deficient RC beams using innovative mortar-based systems. The role of the RC beams' inherent deficiencies as well as the impact of the design parameters of the alternative jacketing configurations were identified. Existing design models proposed to predict the contribution of the mortar-based composites to the shear strength of RC beams were assessed using the database and conclusions were drawn regarding their accuracy.

1. Introduction

Most of the existing reinforced concrete (RC) buildings were designed according to old design standards which often overestimate RC beams' shear strength [1–3]. In addition, poor reinforcement detailing such as insufficient transverse reinforcement (i.e., inadequately anchored, sparse stirrups, smooth bars) and lap-splices in the plastic hinge region increase further their susceptibility by promoting brittle failure modes such as shear failure that may jeopardise the structure's integrity and cause huge property and life losses [1–3]. Furthermore, ageing of materials (e.g. corrosion of the steel reinforcement), the new challenges imposed by climate change accelerate structural deterioration and increase dramatically their susceptibility. Therefore, to maintain the existing building stock, strengthening becomes the only viable solution.

With the development of composite materials, fibre-reinforced polymer (FRP) jacketing has become an effective intervention method in civil engineering projects, and has been widely used to strengthen deficient RC structures worldwide [4]. However, FRP has significant shortcomings mainly related to its epoxy resin matrix, such as the poor performance at high temperatures, non-applicable to wet surfaces, and incompatible with concrete and masonry [5]. To overcome the issues arising by the use of resins, alternative composite systems have been introduced which retain the advantages of FRP applications but use inorganic (mortar-based) binders instead of resin [6].

Based on the type of textile, various mortar-based composite systems have been developed for the shear strengthening of beams. The term Fibre-Reinforced Cementitious Mortar (FRCM) systems is widely used to include the following systems: (i) TRM (Textile-Reinforced Mortar), in which carbon (CFRCM), glass (GFRCM), basalt (BFRCM) textiles are used [7–9]; (ii) PFRCM (PBO-FRCM), in which Poliparafenilen benzobisoxazole (PBO) textiles are utilised [10]; and (iii) SRG (Steel-Reinforced Grout), in which Ultra-High Tensile Strength Steel (UHTSS) textiles are applied [4,11,12] (Fig. 1).

Gonzalez-Libreros et al. [6] collected the experimental results of 89 externally bonded FRCM shear strengthened RC beams and evaluated the effects of geometry and mechanical properties of beams and strengthening systems. In addition, [6] assessed the efficiency of four analytical models in predicting the shear strength of FRCM strengthened RC beams. According to [6], FRCM systems could improve the shear capacity from 3 % to 195 %, with an average of 55 %, and could also change the failure mode of beams from shear to flexural mode. In addition, the effectiveness of the jacket was affected by parameters such as the strengthening configuration, the compressive strength of the

* Corresponding author.
E-mail addresses: evxxl17@nottingham.ac.uk (X. Liu), georgia.thermou@nottingham.ac.uk (G.E. Thermou).

https://doi.org/10.1016/j.istruc.2023.105474
Received 11 January 2023; Received in revised form 6 August 2023; Accepted 27 October 2023
Available online 6 November 2023

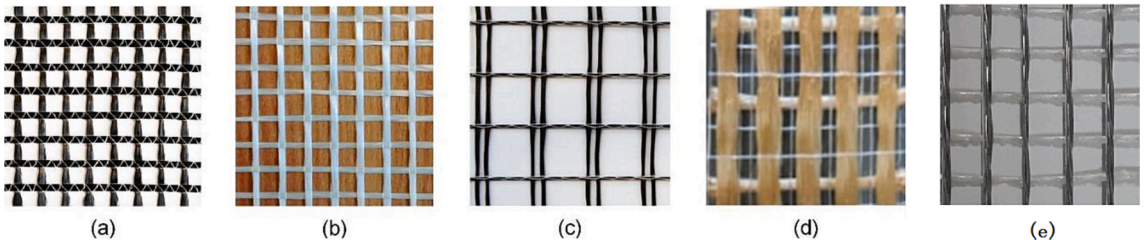

Fig. 1. Textiles used in FRCM jacketing applications: (a) carbon; (b) glass; (c) basalt; (d) PBO; (e) steel textiles.

Table 1
Summary of the studies included in the database.

Reference	SS	f_c'(MPa)	a/d	ρ_w(%)	ρ_f(%)	Number of strengthened beams	Failure mode	
							Shear	Flexural
[11]	FRCM	34.0	1.6–3.1	0.00	0.19, 0.38	8	8	
[18]	FRC	28.3	2.6	0.12	–	1	1	
[24]	FRC	30.0	1.5, 2.5	0.19	2.00	4	4	
[25]	FRC	26.3	2.3, 3.0	0.00	2.00	3	3	
[26]	FRC	30.0	4.5	0.00	0.00–0.015	4	4	
[4]	FRCM	28.0, 23.0	2.2	0.00	0.08–0.25	9	3	6
[10]	FRCM	39.0	2.4	0.27	0.03	9	9	
[12]	FRCM	34.0	2.8	0.27	0.19, 0.38	8	8	
[14]	FRC	32.4, 36.7	2.8	0.11	0.00–1.50	7	7	
[15]	FRC	28.6	1.6	0.89	2.00	2	2	
[16]	FRC	44.8	2.0, 3.0	0	1.50	8	8	
[20]	FRCM	25.8	2.0	0.18	0.12	6	6	
[27]	FRCM	34.0	2.6	0.13	0.15–0.44	8	8	
[28]	FRC	26.6	2.0, 3.0	0	–	4	4	
[29]	FRC	30.0	2.1	0.13	2.0	2	1	1
[30]	FRCM	36.0	2.4	0.27	0.03	4	4	
[31]	FRCM	39.0	2.4	0.27	0.03	1	1	
[9]	FRCM	61.0	3.2	0.00–0.19	–	3	3	
[32]	FRCM	16.8–20.0	1.6–3.6	0.00	0.09–0.60	19	19	
[33]	FRCM	30.0	2.0	0.00, 0.18	0.12, 0.13	6	6	
[34]	FRCM	30.0	1.8	0.00	0.08, 0.13	6	5	1
[35]	FRCM	61.0	1.6	0.00, 0.19	–	2	2	
[36]	FRC	30.0	2.1	0.13	2.0	2	1	1
[13]	FRC	35.0	2.2	0.33	–	3	3	
[23]	FRCM	21.0–25.0	3.3	0.23, 0.33	0.06, 0.36	6	6	
[37]	FRCM	30.0	2.0	0.00	0.06–0.13	15	15	
[38]	FRCM	45.0	2.5	0.00, 0.61	0.02–0.10	6	6	
[8]	FRCM	16.0–18.0	3.2	0.00	1.86–3.80	9	9	
[17]	FRC	24.4–25.2	3.3	0.21	–	5	5	
[39]	FRCM	36.0	3.0	0.00–0.50	1.33, 2.67	6	6	
[40]	FRCM	11.0–20.0	2.3, 2.6	0.00	0.36–0.60	20	19	1
[41]	FRCM	11.0–20.0	1.6	0.00	0.06–0.26	9	10	
[1]	FRCM	38.0	2.2	0.00	–	4	4	
[42]	FRC	26.3	1.8	0.00, 0.30	–	9	9	
Total						218	208	10

matrix relative to the concrete compressive strength and the axial stiffness of the fibre. It was also highlighted that beam's shear strength was improved substantially when the compressive strengths of the matrix and the substrate were similar. Regarding the assessment of existing models to predict the shear strength of the FRCM jacket, it was concluded that the analytical model based on bare fibre characteristics provided more accurate results [6].

Recently, Engineering Cementitious Composites (ECC), Steel Fibre-Reinforced Concrete (SFRC) and Ultra-High Performance Fibre-Reinforced Concrete (UHPFRC) are applied in the form of jackets as externally bonded reinforcement or near surface embedded elements for shear strengthening of deficient RC beams [13–16]. Other hybrid systems developed use FRP grids or welded bar meshes embedded in ECC or other types of cementitious composites like Polymer-Modified Mortar (PMM) or sprayed Polymer-Cement Mortar (PCM) [17,18]. The term ECC-R will be used in the following to describe this last group of hybrid mortar-based composites. To facilitate the descriptions in the following, ECC, UHPFRC, SFRC and ECC-R are collectively referred to as FRC (Fibre Reinforcement Concrete).

Recent studies have confirmed that mortar-based composites system is an effective externally applied reinforcement for RC beams and columns [6,19–22]; however, the studies on the shear behaviour of strengthened RC beams are still limited [23].

In the first part of this paper, a detailed literature review was carried out on the shear performance of RC beams strengthened with mortar-based composite jacketing. A database was compiled and the impact of the design parameters of the beams and the mortar-based composite systems on the shear strength increase was studied. In the second part, existing design models proposed to predict the contribution of the mortar-based composites to the shear strength of RC beams were assessed using the database and conclusions are drawn regarding their accuracy.

2. Experimental database

An overview of the studies considered for the development of the

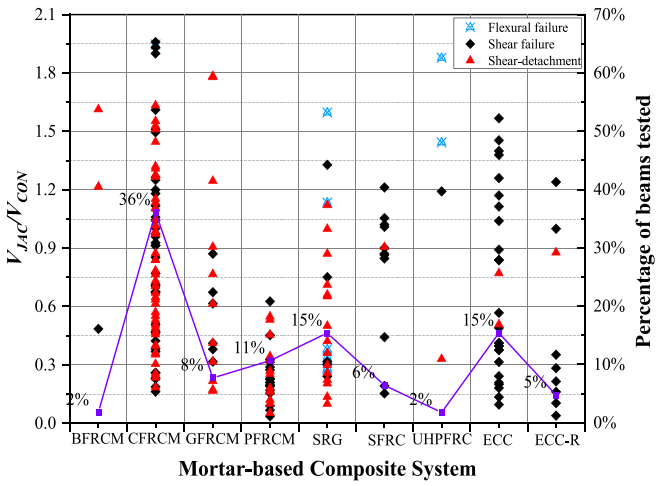

Fig. 2. Variation of V_{JAC}/V_{CON} as a function of the various mortar-based composite systems.

experimental database is presented in Table 1 (218 beams from 36 experimental studies), including FRCM (TRM, PFRCM, SRG) and FRC (SFRC, UHPFRC, ECC, ECC-R) jacketing systems. The literature is sorted based on the publication year, from the most recent (2020) to the oldest (2014). The data range of the strengthening system (SS), the concrete compressive strength (f_c'), the shear span ratio (a/d), the stirrup reinforcement ratio (ρ_w), the web reinforcement ratio of the textile in FRCM and fibres' volume fraction in FRC (ρ_f), as well as the mode of failure as typical parameters influencing shear performance in each literature are also presented in Table 1. The detailed database compiled for the known mortar-based composites is shown in Table A1 of Appendix A.

The database (see Table A1), apart from the details of the beams and the applied mortar-based composites, presents the failure modes observed during testing as well as the shear strength provided by the mortar-based composite jacket V_{JAC} ($= V_{RET} - V_{CON}$; where V_{RET} and V_{CON} are the shear strength of the strengthened and the corresponding reference beam (control beam)). The ratio V_{JAC}/V_{CON} reflects the contribution of the mortar-based composite on the strength increase of the control beams. In the following, graphs are developed which illustrate the impact of the mechanical and geometrical properties of the strengthened beams on V_{JAC}/V_{CON}. The data are grouped based on their mode of failure using the classification proposed by [6]. The shear strengthened beams failed in three distinct modes: i) flexural failure where concrete crushing follows the longitudinal steel bar yielding; ii) shear failure where failure is caused by diagonal tension, fabric rupture, etc.; and iii) shear-detachment where shear failure occurs when detachment occurs either between the composite and the beam substrate or within the mortar layer (mostly in the case of multi-layered composite jackets). In some cases, the application of the mortar-based composite jackets (fully wrapped) modified the mode of failure from brittle to ductile flexural failure. The beams that present flexural failure can be considered as the lower bound of the strengthening capacity [6].

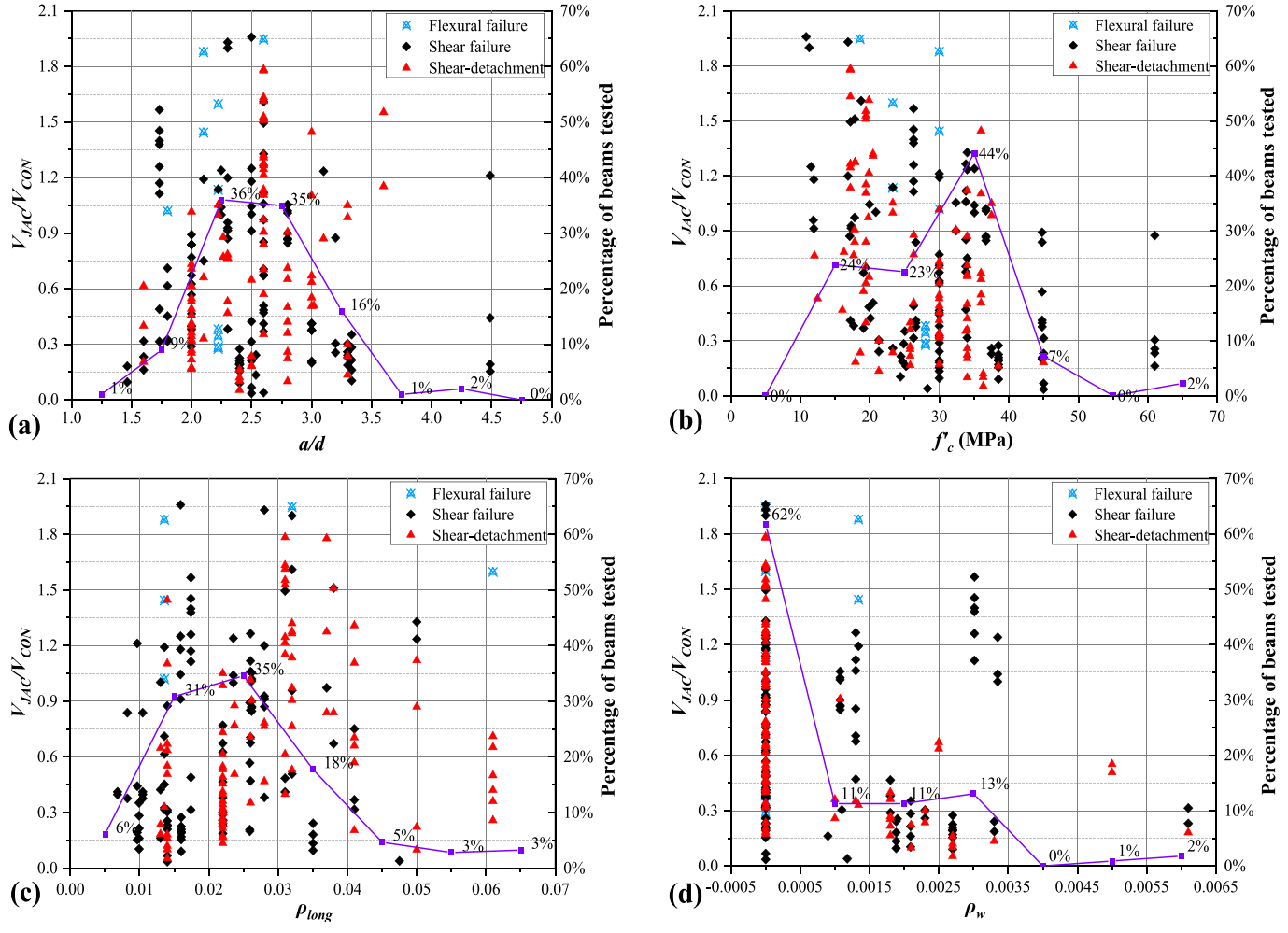

Fig. 3. Variation of V_{JAC}/V_{CON} with (a) a/d, (b) f_c', (c) ρ_{long}, (d) ρ_w.

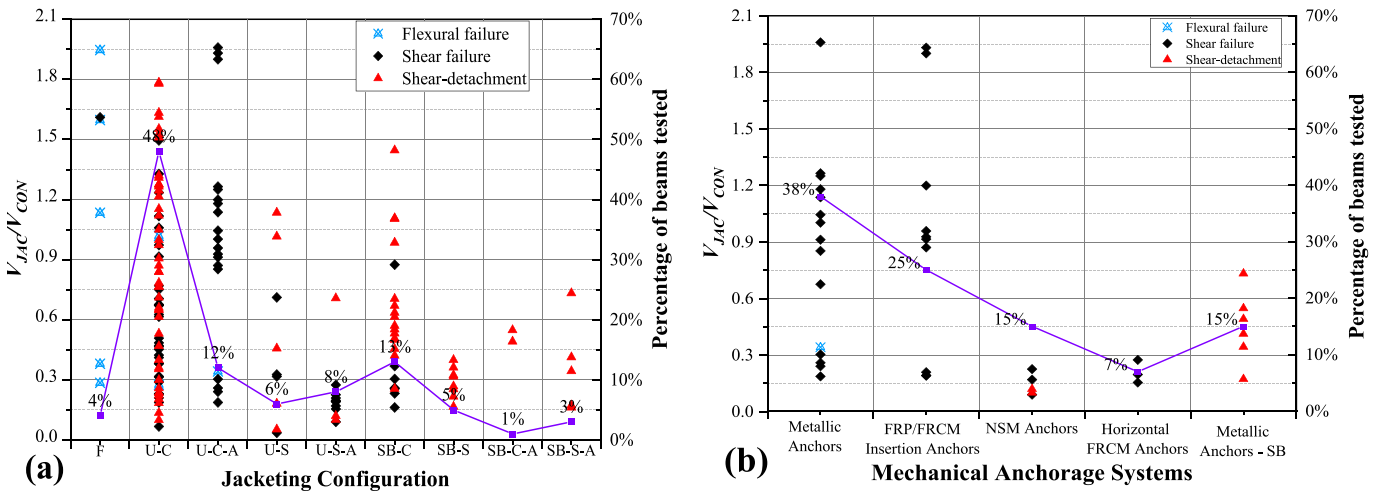

Fig. 4. Variation of V_{JAC}/V_{CON} with (a) jacketing configuration and (b) mechanical anchorage systems.

In general, the addition of mortar-based composite jacketing systems substantially improved the shear behaviour of the RC beams (up to 196 %), as presented in Fig. 2 (The purple curve indicates the percentage of the beams (see the secondary axis) of the database that corresponds to the data related to each abscissa interval). For FRCM systems, the shear strength of RC beam was increased by 61 % on average, 196 % on the maximum and 4 % on the minimum. The average strengthening effect of FRC systems (80 %) was slightly better than that of FRCM system, and the shear strength of RC beam can be increased from 4 % to 190 % in the data collected. There is a large variation of V_{JAC}/V_{CON} depending on the system applied and the mode of failure (Fig. 2). Most of the beams were strengthened using FRCM systems (72 % of the beams of the database) and among them the CFRCM is the dominant one (36 % of the jacketed beams). SRG and ECC systems were applied equally to 15 % of the beams of the database. The less investigated systems seem to be the UHPFRC (2 %), SFRC (6 %) and ECC-R (5 %) jacketing.

2.1. Evaluation of the design parameters of the strengthened RC beams

In this section, the variation of V_{JAC}/V_{CON} as a function of the design parameters of the beams such as the shear span ratio, a/d, the mean cylindrical concrete compressive strength, $f_c^{'}$, the longitudinal steel reinforcement ratio, $\rho_{long}(=A_{sl}/b_w d)$, and the stirrup reinforcement ratio, $\rho_w(=A_w/b_w s)$ (where s is the stirrups spacing; b_w is the beam width; A_{sl} is the sectional area of the tensile reinforcement; A_w is the sectional area of the stirrups) is presented in Fig. 3.

Most of the tested beams have a shear span ratio, a/d, between 2 and 3 (71 %) which corresponds to the 'shear failure valley', that is, the transition zone between shear compression failure and oblique tension failure [43] (Fig. 3(a)). The variation of V_{JAC}/V_{CON} as well as the mode of failure seems to be independent from a/d. The variation of V_{JAC}/V_{CON} with the concrete compressive strength, $f_c^{'}$, is presented in Fig. 3(b). The highest values of strength increase are observed for $f_c^{'}$ values up to 20 MPa (24 %), which are considered representative of old type construction. As observed in Fig. 3(b), there is a trend the effectiveness of the mortar-based composite systems to decrease as the concrete compressive strength increases.

Regarding the reinforcement detailing of the beams, most of the beams (64 %) have a longitudinal steel reinforcement ratio, ρ_{long}, higher than 0.02, which in some cases exceed the maximum reinforcement ratio, ρ_{max}, to avoid flexural failure (Fig. 3(c)). The stirrup reinforcement ratio, ρ_w, seems to influence the effectiveness of the mortar-based composite jackets (Fig. 3(d)). Excluding the case of $\rho_w = 0$ (no presence of stirrups in the shear critical region), for ρ_w values up to 0.0025, which corresponds to beams strengthened with FRCM systems, the effectiveness of the jacket is reduced with the increase of the shear reinforcement (i.e. closely spaced stirrups). This is mainly attributed to the interaction between the internal and external shear reinforcement [6]. The beams with ρ_w between 0.0030 and 0.0035 seem not to follow this trend, which mainly corresponds to the beams strengthened with FRC jackets. A detailed analysis on the impact of the external shear reinforcement FRCM system follows in section 2.2.

2.2. Evaluation of the design parameters of FRCM jacketing systems

2.2.1. Strengthening configuration

The database contains 164 collected beams strengthened by FRCM systems (Table A1 – [1,4,8–12,20,23,27,30–35,37–41]). The variation of V_{JAC}/V_{CON} as a function of FRCM jacket configuration is presented in Fig. 4(a). Regarding the notation given to the alternative jackets, "F" and "U" stand for the fully wrapped and U-shaped jackets, respectively, whereas "SB" for the side bonded. "C" and "S" correspond to continuous textiles and textile strips, respectively. "A" indicates the presence of a mechanical anchorage system. U-shaped jackets were applied to 74 % of the strengthened beams from which 12 % and 48 % used continuous textiles with and without mechanical anchorage, respectively. The rest used textile strips with (8 %) and without mechanical anchorage (6 %). Side bonded jackets with continuous textiles and textiles strips were applied to 14 % and 8 % of the database beams, respectively. By excluding the fully wrapped beams (4 %), in general the U-shaped FRCM jackets seem to be more effective when compared to the side bonded ones. As observed in Fig. 4(a), the most common mode of failure is shear detachment (49 %), which was observed even in the beams that mechanical anchorage was used (23 %).

The mechanical anchorage systems used in 40 [4,8,10,23,27,30,31,37,40,41] out of 164 beams of the database for the application of the FRCM jackets are the following: i) metallic (steel or aluminium) anchors; ii) FRCM/FRP insertion anchors; iii) near surface mounted (NSM) anchors; and iv) horizontal FRCM laminate anchors. Details about the aforementioned mechanical anchorage systems can be found in [44]. Fig. 4(b) presents the relationship between the failure modes of the strengthened beams when the mechanical anchorage systems were adopted. For U-wrapped strengthened beams, except for NSM anchors, the other three methods can improve the adhesion between the FRCM system and the concrete surface. Metallic (steel or aluminium) anchors are an effective method to prevent debonding of the system significantly, but [38] illustrated that it is ineffective in preventing the fibre from sliding in the matrix. No detachment failure mode can be found for FRCM/FRP insertion and horizontal FRCM laminate anchors.

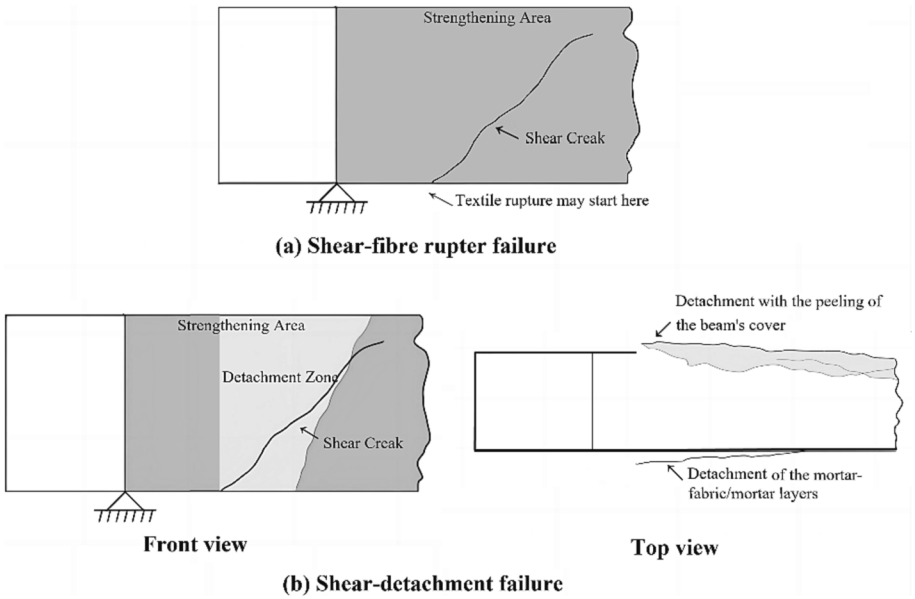

Fig. 5. Failure modes: (a) shear-fibre rupture; (b) shear-detachment.

In the research carried by [8], T-beams strengthened with the 2-layered carbon TRM jacket using FRCM/FRP insertion anchors had similar behaviour to the 4-layered carbon TRM jacketed beams without anchorage system, thus demonstrating the need of using anchorage systems in providing a more cost-effective strengthening solution. However, according to Baggio et al. [6], the use FRCM/FRP insertion anchors in U-shaped FRCM jacketed rectangular beams increased strength by only 3 % compared with beams without anchors. As observed by [16] the lack of effectiveness of such an anchorage system may be related to the fact that the anchors are intended to restrain out-of-plane peeling of the composite and do not restrain the in-plane fibre slippage. Moreover, [6] demonstrated that although beams with and without anchors exhibited diagonal tension shear failure, the presence of anchors slightly changed the inclination of shear cracks around the anchors. In the collected data, only 50 % of the samples with NSM anchorage prevented detachment. It is worth noting that all these detached NSM anchorage samples refer to the U-shaped strip configuration. However, [30] demonstrated that NSM system was still effective compared with the non-anchored ones, since they had higher shear capacity and delayed the occurrence of detachment. The failure mode observed was the gradual crack's development, leading eventually to jacket debonding. In the case of side-bonded jacketing, metallic anchors could not prevent the detachment of the jackets (Fig. 4(b)).

2.2.2. *Failure modes*

The failure modes of the FRCM shear strengthened beams included in the database for the different jacketing configurations are presented in Fig. 4(a). Additionally, Fig. 5 illustrates the typical failure modes attributed to fibre rupture or detachment of the jacket.

Fully wrapped beams: In most cases, failure occurred due to fibre rupture. Although debonding is most likely to happen first, shear capacity is controlled by the rupture of the textile [4,40]. The fully wrapped configuration creates a larger contact area and bonding strength between the jacket and substrate, enhancing the interface friction and transfer of frictional forces between the strengthening system and concrete. Furthermore, the fully wrapped configuration creates a tight wrapping layer that serves as a protective barrier for the concrete surface, reducing the risk of surface delamination and damage. These factors make the mortar-based composite jacket less prone to premature detachment and increase the likelihood of transforming the beam's response from shear to flexural failure. In case of shear failure, noticeable diagonal cracks can be observed on the jacket, especially near the supports and load application points, with fibre rupture commonly occurring at the crack initiation location at the bottom of the beam [46]. Fig. 5(a) illustrates a typical shear failure mode caused by fibre rupture.

U-wrapped beams: Most U-wrapped beams without mechanical anchorage systems failed due to detachment of the composite, which can be further classified as follows: (a) detachment of the textile from the jacket-beam interface accompanied by the peeling of the beam's cover; (b) complete extraction of some fibres in the textile; (c) detachment of the jacket itself accompanied by the detachment of the mortar-fabric/mortar layers or the delaminated or slipped multi-layer textiles. Fig. 5 (b) illustrates the potential detachment mode in this failure scenario, with the left side presenting the frontal view and the right side showing the top view. It is worth noting that in this failure mode, shear diagonal cracks on beams can be observed after the jacket is removed. In general, the detachment of mortar-based composite jacketing does not affect the concrete surface of RC beams [4,8,12], but a few researchers mention that the concrete cover peels off [5,39]. In addition, [37] observed that fibre slippage was more likely to occur in fabrics with higher density since the closely spaced fibres may prevent the uninhibited flow of the mortar, leading thus to a reduced bond quality. The beams failing in this mode often demonstrate significantly constrained ductility [46]. Another key failure mode similar to that of a fully wrapped reinforcement configuration is the rupture of the fibre [27,41]; this appears to be more common in systems with anchors. In the case of U-wrapped jackets with anchors, there is another failure mode in which the anchorage is separated or the surrounding area of the anchorage is damaged [8,10]. This phenomenon is also common in FRP systems [45].

Side bonded beams: Detachment was the mode of failure observed for the side bonded beams. Almost all specimens had 45° diagonal cracks at the load location when failure occurred [20,37]. [37] observed the following detachment patterns: (i) longitudinal stripping of the jacket at the top; (ii) debonding of the jacket in the vertical direction, that is, the detachment along with the whole depth of the beam at the load position; (iii) longitudinal peeling of mortar-based composite system at the bottom; and (iv) the peeling of the jacket in the inclined direction, which is more common on the inclined mortar-based composite system strips. Based on the data collected, anchoring does not have a significant impact on the failure mode of side bonded jackets. Therefore, to avoid premature detachment of the strengthened beams, certain design codes for externally bonded FRP composite materials design prohibit using

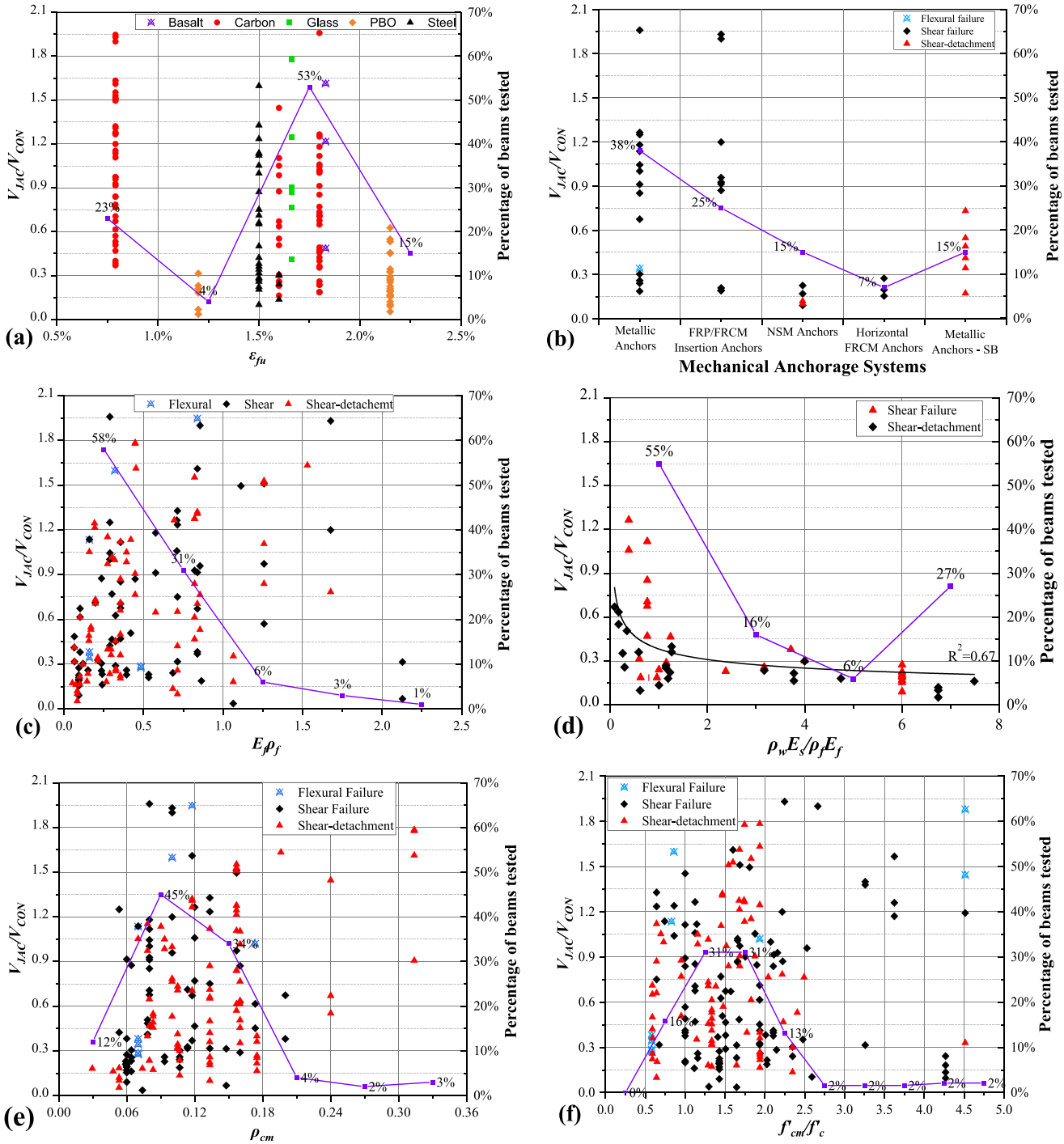

Fig. 6. Variation of V_{JAC}/V_{CON} with (a) ε_{fu}, (b) ρ_f, (c) $E_f\rho_f$, (d) $E_s\rho_w/E_f\rho_f$ (e) ρ_{cm}, (f)f'_{cm}/f'_c

side bonded jackets [46]. Based on the review, this approach may need to be adopted also for the case of FRCM systems.

In addition to the influence of the strengthening configuration on the failure mode, the reinforcement ratio of longitudinal and transverse bars (ρ_{long} and ρ_w) in the beam also has an impact. As shown in Fig. 3(c) and (d), increasing ρ_{long} and ρ_w leads to a slight decrease in the probability of detachment of the strengthening jacket. This decrease can be attributed to the fact that a higher reinforcement ratio enhances the load transfer mechanisms within the beam, thereby reducing localized stress concentrations. This improved load transfer capacity reduces the strain and stress on the strengthening jacket, thereby reducing the risk of detachment. Furthermore, a higher ρ_{long} and ρ_w contributes to better control of deflection and crack development in the beam, which enhances the overall structural integrity and limiting concrete's cover peeling. The reduced deflection also mitigates the discrepancy in load displacement response between the strengthening system and the substrate, thereby further preventing detachment.

2.2.3. *Evaluation of the design parameters of the FRCM system*

The variation of V_{JAC}/V_{CON} with the nominal ultimate strain of the textiles as provided by the manufacturer (ε_{fu}), the web reinforcement ratio of the textile (ρ_f), the axial rigidity of the textile ($E_f\rho_f$), the FRCM reinforcement ratio (ρ_{cm}), and f'_{cm}/f'_c (where f'_{cm} is cementitious matrix compressive strength) is depicted in Fig. 6. The web reinforcement ratio

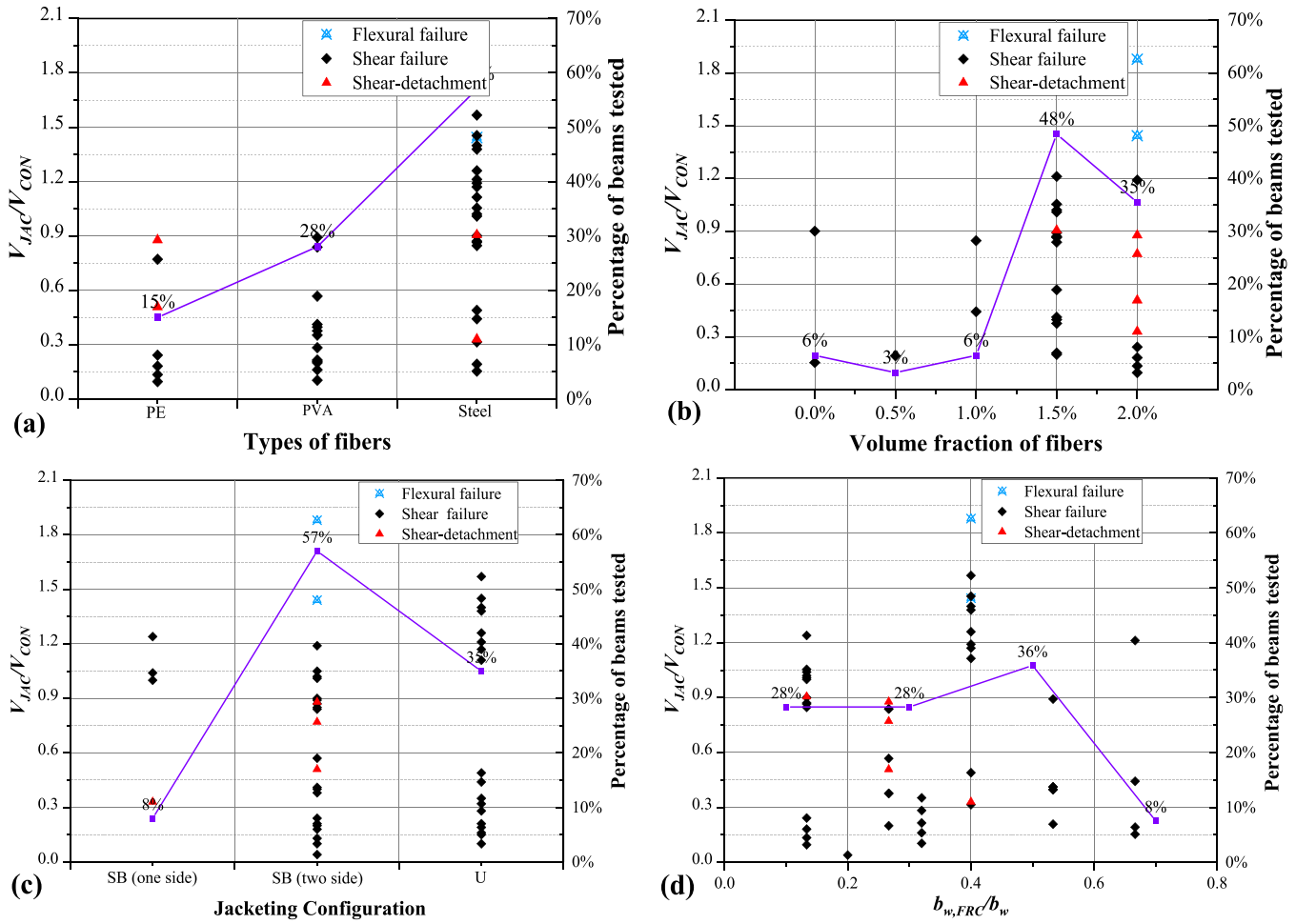

Fig. 7. Variation of V_{JAC}/V_{CON} with (a) fibre type, (b) volume fraction of fibres, and (c) jacketing configuration and (d).$b_{w,FRC}/b'_w$

(ρ_f) and the FRCM reinforcement ratio (ρ_{cm}) are defined as follows [6]:

$$\rho_f = 2nt_f w_f / b_w s_f \quad (1)$$

$$\rho_{cm} = 2t_{cm} w_f / b_w s_f \quad (2)$$

where n is the number of textile layers applied; t_f is the thickness of the textile; $t_{cm}(=(n+1)t_m)$ is the total thickness of the FRCM composite (t_m is the nominal thickness of a single mortar layer);w_f is the width of FRCM strips; and s_f is the longitudinal distance of FRCM strips (if the textiles are applied as continuous, then $w_f = s_f = 1$).

Regarding ε_{fu}, apart from glass and basalt fibre, the rest of the materials have two or more different values for ε_{fu}. Most of the beams (53 %) were strengthened with textiles that had ε_{fu} in the range of 1.5–2.0 % (Fig. 6(a)). 87 % of the strengthened beams had a web reinforcement ratio $\rho_f < 0.0045$ and 48 % had $\rho_f < 0.0015$ (Fig. 6(b)). The variation of V_{JAC}/V_{CON} seems not to be directly related to the amount of web reinforcement confirming similar observations made in other studies [52–54]. The increase of ρ_f has a slight impact on the CFRCM jacket shear strength ($average: V_{JAC}/V_{CON} = 0.86$), a significant impact on the B- and GFRCM jacket shear strength ($average: V_{JAC}/V_{CON} = 1.10 \text{and} 0.69$) and almost no effect on the PFRCM and SRG ($average: V_{JAC}/V_{CON} = 0.25 \text{and} 0.62$).

The interaction between internal transverse steel reinforcement (stirrups) and the externally bonded FRCM jackets has not been studied in detail. Similar to the approach adopted for FRP jacketing [47], the ratio of the axial stiffness of the transverse steel reinforcement to that of the FRCM composite ($E_S\rho_W/E_f\rho_f$; where $E_f\rho_f$, is axial rigidity of the textile index of FRCM composites; E_f is the elastic modulus of the textile fibres in GPa; E_s is the elastic modulus of steel reinforcement) is used to evaluate the interaction between stirrups and the FRCM system. In Fig. 6 (c) and (d), the relationship between $E_f\rho_f$ and $E_S\rho_W/E_f\rho_f$ with V_{JAC}/V_{CON} is presented, respectively. The $E_f\rho_f$, which expresses the axial rigidity of the textile, for most of the jackets lies between 0.052 and 1 (89 % of the beams). For similar axial rigidity values, the PFRCM system seems less effective than the rest of the FRCM systems (C-, G-, BFRCM and SRG). When internal shear reinforcement is present (Fig. 6(d)), the increase of $E_S\rho_W/E_f\rho_f$ (i.e., more stirrups for the beam) renders the contribution of the FRCM system less effective. Using the experimental data shown in Fig. 6(d), and after applying exponential curve fitting to the data (51 beams), the following empirical expression is derived:

$$V_{FRCM}/V_{CON} = 0.383\left(E_s\rho_w/E_f\rho_f\right)^{-0.3} \quad (3)$$

Eq. (3) should be treated with caution since it is based on a limited amount of data.

Regarding the FRCM reinforcement ratio, most of the specimens (79 %) receive ρ_{cm} values between 0.06 and 0.18 (Fig. 6(e)). In general, the increase of ρ_{cm} leads to increased shear capacity for the beams. This is attributed to the fact that an increase in ρ_{cm} corresponds to an increase in the thickness of the FRCM mortar, which increases the cross-sectional area (especially the width) of the RC beam, thereby improving the shear capacity of the beam. The impact of the cementitious matrix compressive strength, f'_{cm}, on V_{JAC}/V_{CON} is presented in Fig. 6(f). 91 % of the studies used f'_{cm}/f'_c between 0.5 and 2.5. As observed in the Fig. 6(f),

Table 2
Analytical models for the shear strength contribution of the FRCM jacket based on fibre properties.

Reference	V_{FRCM}
Model 1 [51]; Model 2 [52]*	$V_{FRCM} = 2nt_f h_f \frac{w_f}{s_f}\varepsilon_{eff}E_f(cot\theta + cot\alpha)sin\alpha V_{FRCM} = 2nt_f h_f \frac{w_f}{s_f}\varepsilon_{eff}E_f;\ \theta = 45^0; \alpha = 90^0$ For [51]:$\varepsilon_{eff} = 0.5\varepsilon_{fu}$ For [52]: For fully wrapped: $\varepsilon_{eff} = 0.035\left(\frac{f_c^{'2/3}}{\rho_f E_f}\right)^{0.65}\varepsilon_{fu}$ For side bonding or U-wrapped:$\varepsilon_{eff} = 0.020\left(\frac{f_c^{'2}}{\rho_f E_f}\right)^{0.55}\varepsilon_{fu}$ Experimental value of effective strain:$\varepsilon_{eff}^{exp} = \frac{V_{FRCM}^{exp}}{2nt_f h_f (w_f/s_f)E_f}$
Model 3 [7] **	$V_{FRCM} = 2nt_f b_w h_f \frac{w_f}{s_f} f_{fed}(cot\theta sin\alpha + cos\alpha);$ $V_{FRCM} = 2nt_f b_w h_f \frac{w_f}{s_f} f_{fed};\ \theta = 45^0; a = 90^0; f_{fed} = D_f f_{fed,max} f_{fed,max} = 8.67\beta_l\beta_w\sqrt{\frac{1000\sqrt{f_c'}}{nt_f}};\ \beta_l = \begin{cases} 1, \lambda \geq 1 \\ \sin\left(\frac{\pi\lambda}{2}\right), \lambda < 1 \end{cases};\beta_w = \sqrt{\frac{2 - w_f/(s_f sin\alpha)}{1 + w_f/(s_f sin\alpha)}}$ $D_f = \begin{cases} \frac{2}{\pi\lambda}\left(\frac{1 - \cos(\frac{\pi\lambda}{2})}{\sin(\frac{\pi\lambda}{2})}\right), \lambda \leq 1 \\ 1 - \frac{\pi - 2}{\pi\lambda}, \lambda > 1 \end{cases};\ \lambda = L_{max}/L_e$ $L_{max} = \begin{cases} h_f/sin\alpha, \text{for U-wrapped jackets} \\ h_f/2sin\alpha, \text{for side bonding jackets} \end{cases};\ L_e = 15\sqrt{\frac{1000nt_f}{\sqrt{f_c'}}}$ $h_{fe} = z_b - z_t;\ z_b = h_f - (h - d_{fb});\ z_t = d_{ft}$

* n is the number of textile layers applied; t_f is the thickness of fibre sheets; h_f is the effective depth of the jacket taken as 0.9d; w_f is the width of FRCM strips; s_f is the longitudinal distance of FRCM strips; ε_{eff} is the fibre effective strain; E_f is the elastic modulus of the fabric; α is the angle between the fibres and the beam axis perpendicular to the shear force; θ is the angle between the concrete compression strut and the beam axis perpendicular to the shear force.
** D_f is the stress distribution coefficient; $f_{fed,max}$ is the maximum design stress of the jackets; β_l and β_w reflect the effect of the effective bond length and the concrete width ratio of the jacket; λ is the maximum bond length parameter; L_{max} and L_e are the available bond length and the effective bond length respectively; z_b and z z_t are the co-ordinates of the top and bottom ends of the effective FRCM; d_{fb} is the distance from the compression face to the top edge of the FRCM; d_{ft} is the distance from the compression face to the lower edge of the jacket.

Table 3
Analytical models for the shear strength contribution of the FRCM jacket based on FRCM composite properties.

Reference	V_{FRCM}
Model 4 [53]*	$V_{FRCM} = nA_f f_{fv} h_f;$ $A_f = 2t_f w_f/s_f;\ f_{fv} = E_{FRCM}\varepsilon_{eff};\ \varepsilon_{eff} = \varepsilon_{FRCM} \leq 0.004$ Experimental value of effective strain:$\varepsilon_{eff}^{exp} = \frac{V_{FRCM}^{exp}}{nA_f E_{FRCM} d}$
Model 5 [54] **	$V_{FRCM} = k_e\varepsilon_{eff}E_{FRCM}\rho_f b_w d(cot\theta + cot\alpha)sin\alpha;$ $V_{FRCM} = k_e\varepsilon_{eff}E_{FRCM}\rho_f b_w d;\ \theta = 45^0; \alpha = 90^0;$ $\varepsilon_{eff} = \frac{f_{fdd}}{E_{FRCM}}\left[1 - \frac{1}{3}\frac{l_e sin\alpha}{\min(0.9d; h_f)}\right];\ f_{fdd} = \frac{0.24}{\gamma_{fd}\sqrt{\gamma_c}}\sqrt{\frac{E_{FRCM}k_b\sqrt{f_{ck}'f_{ctm}'}}{t_f}};$ $f_{ctm}' = 0.30 f_{ck}^{'2/3} k_b = \left(\frac{2 - w_f/b}{1 - w_f/400}\right)^{0.5};\ l_e = \left(\frac{E_{FRCM}t_f}{2f_{ctm}'}\right)^{0.5};\ k_e = 0.5$ $b = \begin{cases} s_f, for strips \\ 0.9d\sin(\theta + \alpha)/sin\alpha, for continous \end{cases};$ Experimental value of effective strain:$\varepsilon_{eff}^{exp} = \frac{V_{FRCM}^{exp}}{k_e E_{FRCM}\rho_f b_w d}$
Model 6 [37] ***	$V_{FRCM} = F_z(V_m + V_f);$ $F_z = \frac{Nw_f}{a}V_m = 2(0.17\sqrt{f_{cm}'}t_m d);\ V_f = 2nA_f f_{fv} d f_{fv} = E_{FRCM}\varepsilon_{eff};$ $\varepsilon_{eff} = \varepsilon_{FRCM} \leq 0.004$ Experimental value of effective strain:$\varepsilon_{eff}^{exp} = \frac{(V_{FRCM}^{exp}/F_z - V_m)}{2nA_f E_{FRCM} d}$

* A_f is area of mesh reinforcement by unit width; f_{fv} is design tensile strength of the FRCM system.
** k_e is the "effectiveness coefficient", take 0.5; f_{fdd} is debonding strength; f_{ck}' is concrete characteristic cylindrical strength; f'_{ctm} is average tensile strength of concrete; γ_{fd} and γ_c are partial safety factor, which are taken as 1 in this chapter; k_b is the geometric coefficient; l_e is optimal bond length.
*** V_m and V_f are shear strength contribution from textile and mortar, respectively; F_z is the ratio of the total length of the strengthened zone to the critical shear span; N is number of FRCM strips; a is the length of shear critical span.

there is not direct correlation between f_{cm}'/f_c' to V_{JAC}/V_{CON}.

2.3. Evaluation of the design parameters of FRC jacketing systems

The database presented in Table A1 contains 54 collected beams strengthened by the FRC (ECC, ECC-R, SFRC and UHPFRC) systems [13–18,24–26,28,29,36,42]. Fig. 7(a) and (b) present the variation of V_{JAC}/V_{CON} with the fibre type and the fibres' volume fraction. Since some studies do not provide information on the specific fibre types and volume fractions, only the specimens for which full details are provided are presented in Fig. 7(a) and (b) (46 and 31 beams were used in Fig. 7 (a) and (b), respectively). Most FRC systems use steel fibres (57 %), followed by PVA and PE fibres (28 % and 15 %, respectively). A smaller percentage of FRC jacketed beams, especially in the cases that steel or PVA fibres are used, fails due to detachment compared with FRCM strengthened beams. [48] demonstrated that the FRC system can offer a better bonding effect with the beam surface to prevent the occurrence of partial detachment. As seen in Fig. 7(a), the shear strength increases for PE, PVA and steel fibre systems ranges between 5 % and 88 %, 10 % to 89 % and 15 % to 187 %, respectively. Most studies use a volume fraction of fibres between 1.5 and 2.0 % (83 % of the samples in Fig. 7 (b)). Although the number of specimens is small, it seems that there is a trend between the increase in strength as the volume fraction of fibres increases.

Fig. 7(c) shows the variation of V_{JAC}/V_{CON} with the type of jacketing configuration. The most common strengthening configuration in FRC system is side bonding (SB), which accounts for 65 % of the beams, whereas 8 % correspond to one side bonding and the rest (57 %) to two side bonding. SB (two sides) jackets have a greater potential to improve shear strength, and V_{JAC}/V_{CON} increase by up to187%, while for SB (one side) jackets, the strength increased ranges between 33 % and 124 %. For U-wrapped beams (35 % of the samples), V_{JAC}/V_{CON} ranges from 13 to 157 %.

The impact of the ratio of the width of the jacket to the width of the beam, $b_{w,FRC}/b_w$, on V_{JAC}/V_{CON} is presented in Fig. 7(d). The term $b_{w,FRC}$ refers to the width of the mortar-based composite jacket, which corresponds to the total width of the two sides. 64 % of the studies used $b_{w,FRC}/b_w$ between 0.2 and 0.6. Detachment failure is observed for $b_{w,FRC}/b_w$ less than 0.4. Due to the limited number of data and the large dispersion of the results no solid conclusions can be drawn about the impact of $b_{w,FRC}$ on the shear strength increase.

3. Shear resistance of beams retrofitted with mortar-based composites

3.1. Analytical models for FRCM jacketing systems

The total shear strength of FRCM strengthened RC beams (V_{shear}) comprises shear strength contributions from concrete (V_C), steel stirrups (V_s) and FRCM jacket (V_{FRCM}) [49]:

Table 4
Results of the assessment of the analytical models 1–6 based on the selected statistical indices.

Type	Formula	Failure mode	Number	$v_{FRCM}^{exp}/v_{FRCM}^{pred}$			$v_{FRCM}^{pred}/v_{FRCM}^{exp}-1$	
				μ	SD	COV	MAE	RMSE
Fibre-properties- based	Model 1 [51]	No detachment	20	0.60	0.35	0.58	1.22	1.58
		Detachment	75	0.84	1.06	1.26	1.95	3.21
		Total	95	0.79	0.96	1.19	1.80	2.95
	Model 2 [52]	No detachment	20	1.19	0.82	0.69	0.49	0.54
		Detachment	75	3.12	2.02	0.65	0.67	0.93
		Total	95	2.71	1.98	0.73	0.64	0.87
	Model 3 [7]	No detachment	20	0.58	0.19	0.32	0.99	1.16
		Detachment	75	0.70	0.41	0.59	1.09	1.68
		Total	95	0.67	0.38	0.57	1.09	1.60
Composite-properties-based	Model 4 [53]	No detachment	14	2.12	2.80	1.32	1.00	2.01
		Detachment	45	2.61	1.30	0.50	0.54	0.58
		Total	59	2.50	2.05	0.83	0.65	1.10
	Model 5 [54]	No detachment	14	1.78	0.87	0.49	1.08	2.54
		Detachment	45	2.36	0.90	0.38	0.52	0.56
		Total	59	2.22	0.91	0.41	0.65	1.33
	Model 6 [37]	No detachment	14	1.05	2.80	2.67	1.43	3.32
		Detachment	45	1.61	0.93	0.58	0.60	0.74
		Total	59	1.47	2.05	1.39	0.79	1.74

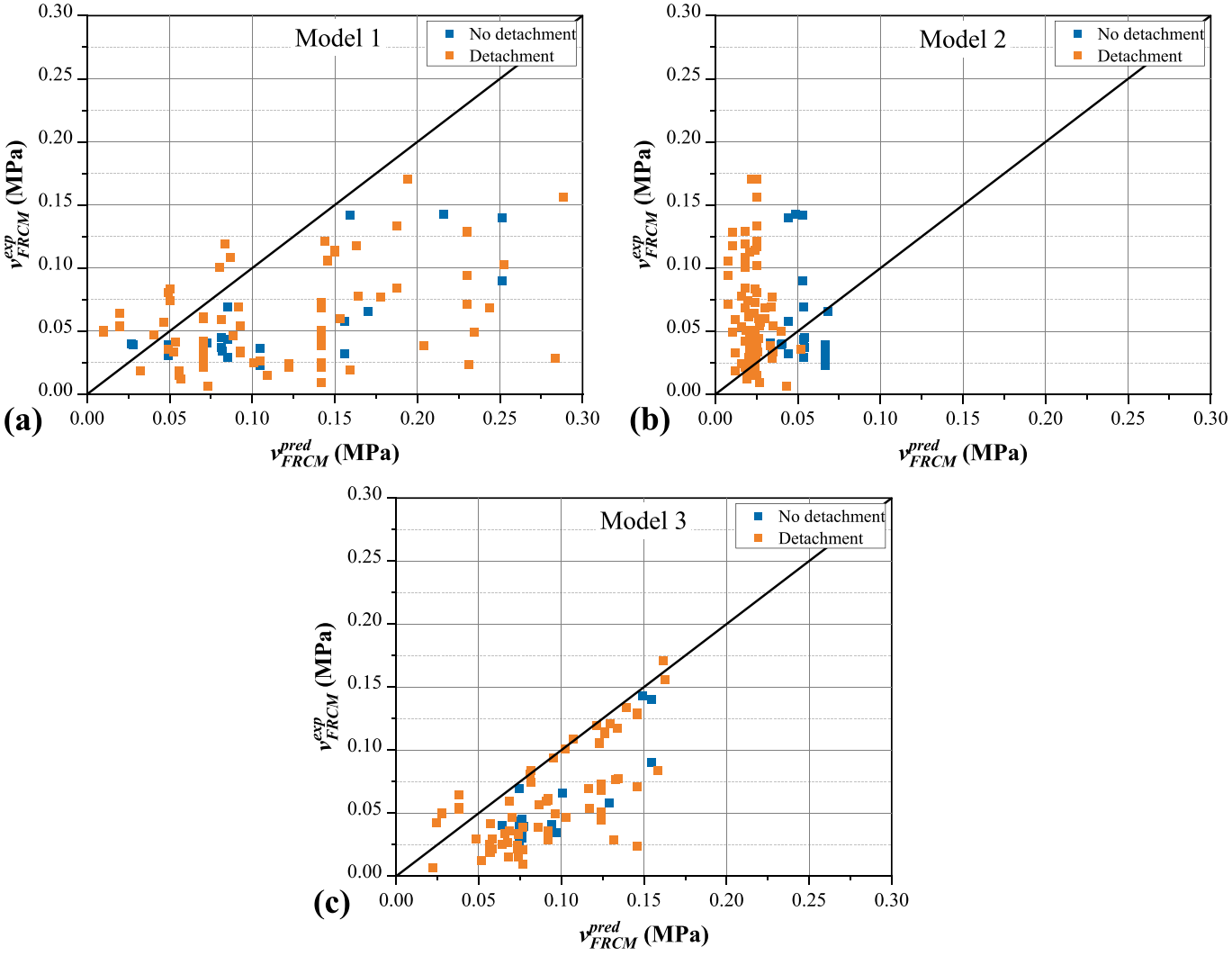

Fig. 8. Comparison between experimental, v_{FRCM}^{exp}, and predicted, v_{FRCM}^{pred}, shear strength for: (a) Model 1; (b) Model 2; (c) Model 3.

$$V_{shear} = V_C + V_s + V_{FRCM} \leq V_{Rd,max} \quad (4)$$

V_{shear} shall not exceed the shear limit value ($V_{Rd,max}$), which corresponds to the crushing of diagonal compression columns in the web of the member [49].

According to EC2 [49] and ACI 318[50], the shear strength

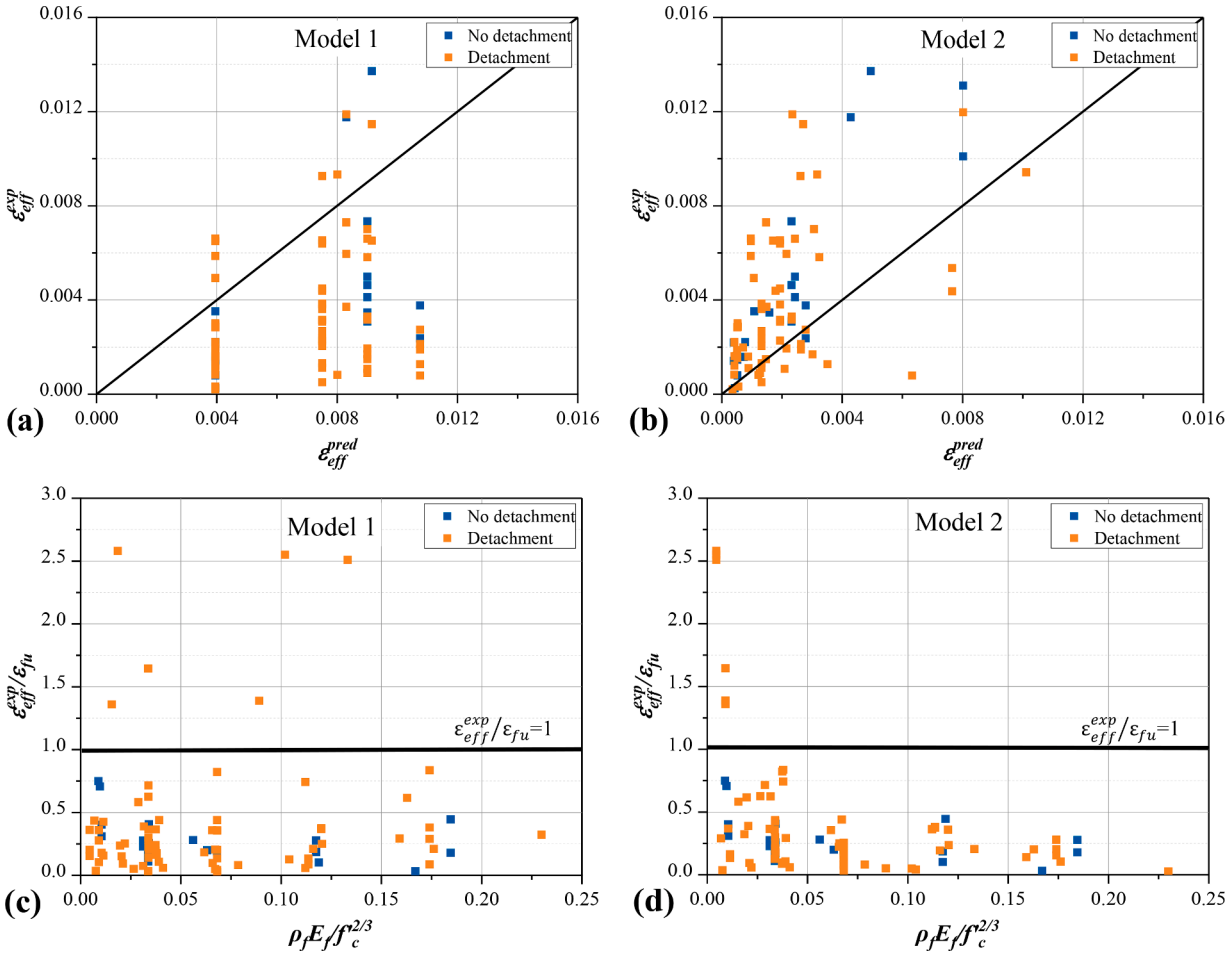

Fig. 9. ε_{eff}^{exp} versus ε_{eff}^{pred}: (a) Model 1, (b) Model 2; Normalized experimental effective strain, $\varepsilon_{eff}^{exp}/\varepsilon_{fu}$ versus $\rho_f E_f/f_c'^{2/3}$: (c) Model 1, (d) Model 2.

contribution from concrete (V_C) is:

$$V_C^{EC2} = 0.12k\left(100\rho_{long}f_c'\right)^{1/3}b_w d$$

$$\geq 0.035k^{3/2}f_c'^{2/3}b_w d \quad (5)$$

$$V_C^{ACI} = 0.167\sqrt{f_c'}b_w d \quad (6)$$

where f_c' is the concrete compressive strength, b_w is the width of the cross-section, d is the depth of the cross-section, ρ_{long} is the area ratio of the tensile reinforcement, and $k = 1+\sqrt{(200/d)} \leq 2.0$(with d in mm) is a factor that considers the size effect. According to EC2 [49], the shear strength contribution from stirrup (V_s) can be calculated as:

$$V_s = \frac{A_w}{s} z f_{ywd} \quad (7)$$

where f_{ywd} is the design yield strength of the shear reinforcement, A_w is the shear reinforcement area, $z = 0.9d$ is the inner lever arm, and s is the stirrup spacing.

The shear strength contribution of the FRCM jacket, V_{FRCM}, can be calculated using the analytical models presented in Tables 2 and 3. The models presented in Table 2 are based on the fibre properties [7,51,52], whereas the models of Table 3 are based on the FRCM composite properties [37,53,54]. The analytical models were implemented in the database presented in Table A1. For all the beams of the database, the angle between the concrete compression strut and the beam axis is perpendicular to the shear force is considered $\theta = 45^0$, whereas the angle between the fibres and the beam axis is perpendicular to the shear force in all the applications is $\alpha = 90^0$. In addition, the expression for the each model's experimental value of the effective strain (ε_{eff}^{exp}) that is calculated from the experimental shear strength appears in Tables 2 and 3, except for Model 3 which does not depend on ε_{eff}^{exp}. Due to limitations imposed by the analytical models, the strengthened beams with anchorage systems and/or flexural failure are not considered in the analysis [6,7,51,52].

The experimental and the predicted normalised shear stress of the FRCM jacketing system, v_{FRCM}^{exp} and v_{FRCM}^{pred}, are calculated from:

$$v_{FRCM}^{exp} = \frac{V_{FRCM}^{exp}}{b_w d f_c'};\ v_{FRCM}^{pred} = \frac{V_{FRCM}^{pred}}{b_w d f_c'} \quad (8)$$

where $V_{FRCM}^{exp}(= V_{JAC}$ see Table A) is the experimental shear strength provided by FRCM jackets; V_{FRCM}^{pred} is predicted the shear strength provided by FRCM jacket which is calculated by the different models.

3.1.1. Assessment of the analytical models for FRCM jacketing systems

The accuracy of the six models in predicting the shear strength of the composite system is assessed using the following statistical indices: the Average Value (μ), Standard Deviation (SD) and Coefficient of Variation (COV) of $v_{FRCM}^{exp}/v_{FRCM}^{pred}$, Mean Absolute Error (MAE) and Root Mean Square Error (RMSE) between v_{FRCM}^{exp} and v_{FRCM}^{pred}. The calculated μ, SD, COV, RMSE, and MAE values for the models are presented in Table 4. COV, MAE and RMSE are calculated as follows:

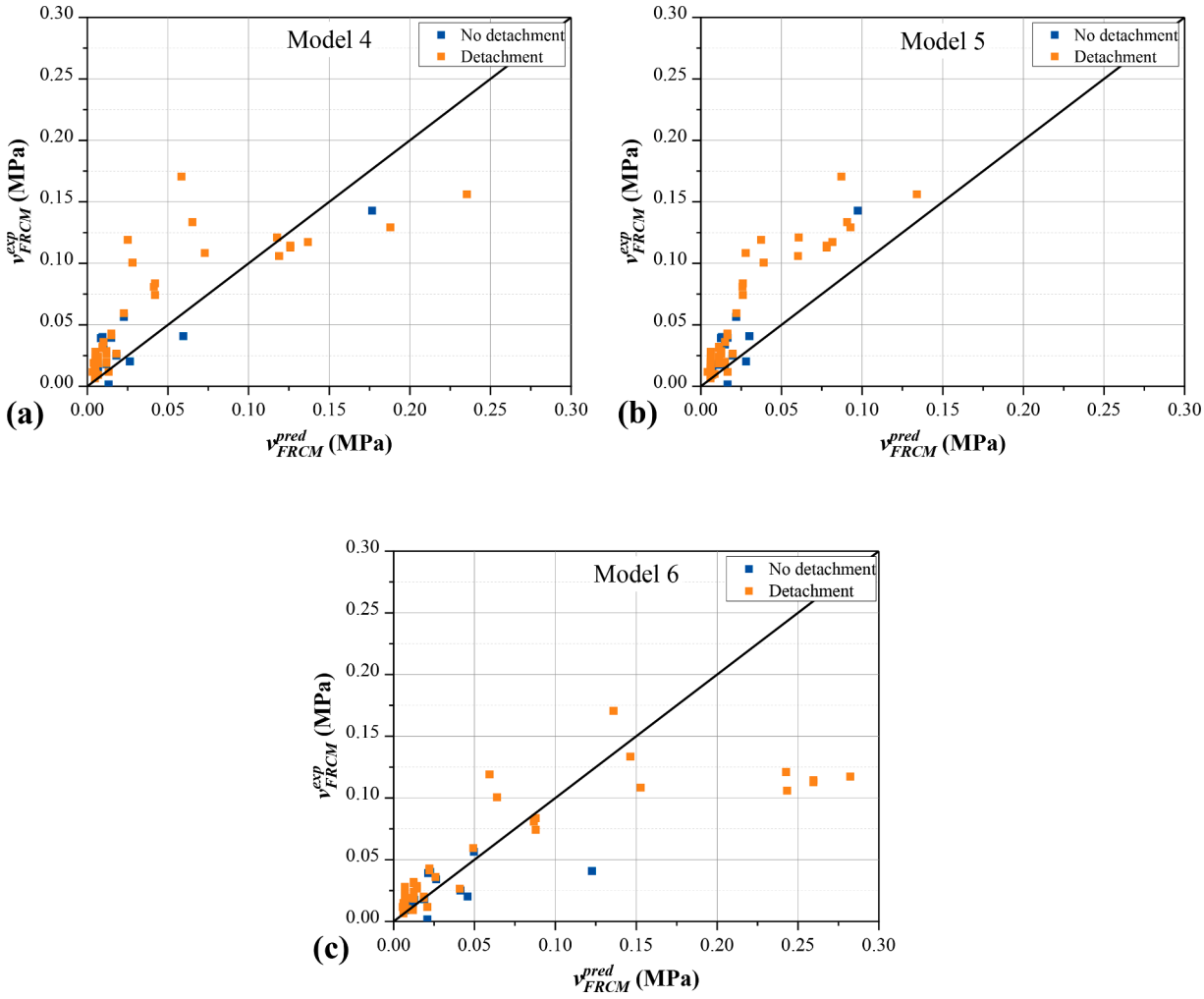

Fig. 10. Comparison between experimental, v_{FRCM}^{exp}, and predicted, v_{FRCM}^{pred}, shear strength for: (a) Model 4; (b) Model 5; (c) Model 6.

$$COV = \frac{SD}{\mu} \tag{9}$$

$$MAE = \frac{\sum_{i=1}^{x} \left| v_{FRCM}^{pred} / v_{FRCM}^{exp} - 1 \right|}{N} \tag{10}$$

$$RMSE = \sqrt{\frac{\sum_{i=1}^{x} \left(v_{FRCM}^{pred} / v_{FRCM}^{exp} - 1 \right)^2}{N}} \tag{11}$$

3.1.1.1. Models based on fibre properties. Triantafillou and Papanicolaou proposed Model 1 [51] for fully wrapped rectangular beams firstly, which was later extended to include U-wrapped beams [6]. However, Model 1 did not consider the impact of jacket detachment on shear performance. To address this, Escrig et al. [52] improved Model 2, which incorporated different expressions for ε_{eff} depending on the presence of the jacket's detachment. In addition, Tetta and Triantafillou [7] proposed Model 3, which eliminated the need for the fibre elastic modulus E_f in the formula. This modification overcame the difficulty of selecting an appropriate elastic modulus value when predicting the shear strength provided by FRCM. Fig. 8 illustrates the relationship between v_{FRCM}^{pred} and v_{FRCM}^{exp} obtained by Models 1 [51], 2 [52], and 3 [7]. As illustrated in Fig. 8(a), the shear strength contribution of the FRCM system in Model 1 is overestimated ($\mu = 0.79$, SD = 0.96, COV = 1.19, Table 4), regardless of whether the strengthening beam fails or not due to the detachment of the FRCM jacket, which would lead to an unsafe situation in shear design. Moreover, the MAE and RMSE of this mode are the largest of all models, reaching 1.80 and 2.95, respectively. For Model 2, the average $v_{FRCM}^{exp}/V_{FRCM}^{pred}$ ratio, SD, and COV are 2.71, 1.98, and 0.73, respectively (Table 4). In contrast to Model 1, Model 2 underestimates the shear contribution of FRCM jacketing for both modes of failure (Fig. 8(b)). This implies that the structure is safe, however the design is not efficient leading to waste of materials and higher cost. Considering the average value of $v_{FRCM}^{exp}/v_{FRCM}^{pred}$ for the two modes of failure (1.19, 3.12 for detachment and non-detachment failure, respectively), in case of detachment Model 2 is less accurate. The average value of $v_{FRCM}^{exp}/v_{FRCM}^{pred}$ for Model 3 is the smallest (0.67) among the 3 models, leading to an overestimation of the strength which is unconservative. However, the predicted values for the CFRCM strengthened beams that failed due to detachment are very close to the experimental ones (Fig. 8(c)).

Fig. 9 presents the experimental value of the fibre effective strain ε_{eff}^{exp} versus the predicted value of strain ε_{eff}^{pred}, as well as the normalized experimental value of effective strain $\varepsilon_{eff}^{exp}/\varepsilon_{fu}$ versus $\rho_f E_f / f_c'^{2/3}$, for Models 1 and 2. Model 3 is not included since it is not based on ε_{eff}. Regarding ε_{eff}^{exp} versus ε_{eff}^{pred}, the effective strain of most beams in Model 1 is underestimated (Fig. 9(a)), which implies that ε_{eff} should be larger than 0.5 ε_{fu}. Although Model 2 used more detailed equations for ε_{eff}, the predicted values of effective strain are underestimated. Therefore, further improvement of the formulae for the effective strain prediction is required. As shown in Fig. 9(c) for Model 1, $\varepsilon_{eff}^{exp}/\varepsilon_{fu}$ has a remarkably decreasing trend as $\rho_f E_f / f_c'^{2/3}$ increases. However, the direct relationship

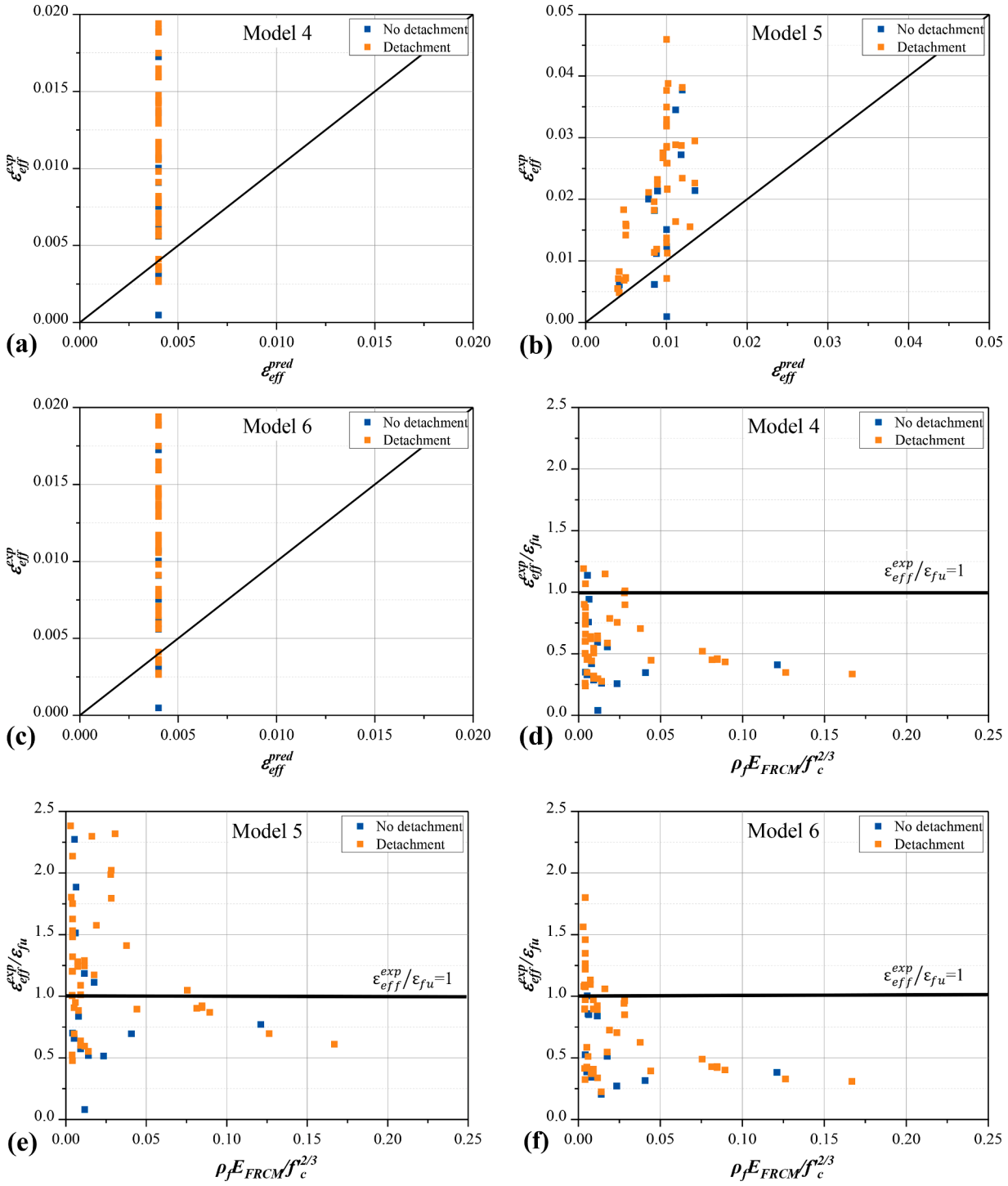

Fig. 11. ε_{eff}^{exp} verse ε_{eff}^{pred}: (a) Model 4, (b) Model 5, (c) Model 6; Normalized experimental effective strain, $\varepsilon_{eff}^{exp}/\varepsilon_{fu}$, versus $\rho_f E_{FRCM}/f_c'^{2/3}$: (d) Model 4, (e) Model 5, (f) Model 6.

between the two variables is not clear due the large dispersion of the results. The trend in Model 2 between $\rho_f E_f/f_c'^{2/3}$ and $\varepsilon_{eff}^{exp}/\varepsilon_{fu}$ compared to that of Model 1 seems to be more consistent (Fig. 9(d)), especially in the case of detachment failure. As observed in both graphs in Fig. 9(c) and (d), for a small number of beams (6.3 % and 5.2 % in Model 1 and 2, respectively) $\varepsilon_{eff}^{exp}/\varepsilon_{fu}$ exceeds 1, which implies that the effective strain is larger than the rupture strain which is not realistic since ε_{eff}^{exp} should be a portion of ε_{fu}. This is attributed to the fact that ε_{eff}^{exp} is not measured but it results after the implementation of Models 1 and 2 for $V_{FRCM}^{exp}(=V_{JAC}$see Table A).

In summary, Model 1 [51] consistently overestimates the shear strength contribution, regardless of whether the FRCM jacket is detached or not. It has the highest Mean Absolute Error (MAE) and Root Mean Square Error (RMSE) values compared to the other two models, indicating a significant deviation from experimental results. Model 3 [7] also tends to overestimate the strength, but the difference between the predicted and tested results is less pronounced compared to Model 1. On the other hand, Model 2 [52] underestimates the shear contribution of

Table 5
Analytical models to predict..V_{FRC}

	Formula
Model 7 [55]*	$V_{FRC} = \frac{2}{3} f_{ct,FRC} \left(\frac{a}{d}\right)^{0.25} b_{w,FRC} d_{FRC}$
Model 8 [56]**	$V_{FRC} = 0.18 b_{w,FRC} d_{FRC} k \left[100 \rho_{long} \left(1 + 7.5 \frac{f_{Ftuk}}{f_{ct,FRC}}\right) f'_{c,FRC}\right]^{1/3}$
Model 9 [57]***	$V_{FRC} = V_{c,FRC} + V_{f,FRC} = \frac{0.18\sqrt{f'_{c,FRC}} b_{w,FRC} d_{FRC}}{\gamma_b} + \frac{(f_{vd,FRC}/\tan\alpha) b_{w,FRC} z}{\gamma_b}$

*Where $f_{ct,FRC}$ is the tensile strength of FRC jacket, taken as $0.3 f'^{2/3}_{c,FRC}$; $f'_{c,FRC}$ is the compressive strength of FRC jacket; $b_{w,FRC}$ is the width of the jacket; d_{FRC} is the effective depth of the jacket;
**k is the is the size effect factor, taken as $1 + \sqrt{200/d_{FRC}} \leq 2.0$; f_{Ftuk} is the characteristic value of the final residual tensile strength of FRC obtained from the crack opening (1.5 mm), and $f_{Ftuk}/f_{ct,FRC}$ would be taken as 0.62 [58];
***where $V_{c,FRC}$ is shear strength contributions from concrete in FRC; $V_{f,FRC}$ is shear strength contributions from fibre in FRC; Where $f_{vd,FRC} = 0.3 f^{2/3}_{c,FRC}/\gamma_c$ is the design average tensile strength perpendicular to diagonal cracks.

Table 6
Results of the assessment of the analytical Models 7–9 based on the selected statistical indices.

Model	Number	$v^{exp}_{FRC}/v^{pred}_{FRC}$			$v^{pred}_{FRC}/v^{exp}_{FRC} - 1$	
		μ	SD	COV	MAE	RMSE
Model 7 [55]	39	1.11	0.84	0.76	1.20	1.86
Model 8 [56]	39	1.63	1.11	0.68	0.63	0.82
Model 9 [61]	39	1.13	0.85	0.75	1.10	1.61

FRCM. However, its prediction results are inaccurate, as both the MAE and RMSE values are larger than those of Model 2. This implies that the structure designed by Model 2 [52] is considered safe, but the design is inefficient, resulting in unnecessary material waste and higher costs.

3.1.1.2. Models based on FRCM composite properties. Since many of the studies included in the database do not provide information on the elastic modulus of the FRCM composite, only 59 beams from the database are used to compare the experimental, v^{exp}_{FRCM}, with the predicted shear stress values, v^{pred}_{FRCM}, using Models 4–6 (Table 3) as shown in Fig. 10.

Model 4 is provided by ACI 549.4R-13 [53], which is only standard considering the shear strength contribution of continuous FRCM U-wrapped or fully wrapped systems. However, it is based on very few experimental tests, and the guidelines also point out that these equations need further validation [6]. As observed in Table 3, Model 4 reaches average $v^{exp}_{FRCM}/v^{pred}_{FRCM}$ ratio (μ) of 2.50, SD of 2.05, and COV of 0.83. Fig. 10(a) demonstrates that Model 4 underestimates the predicted shear strength. This may be attributed to the low value of the effective strain of the fibre considered (limited to $\varepsilon^{pred}_{eff} = 0.004$, see also Fig. 11(a) where ε^{exp}_{eff} is compared to ε^{pred}_{eff}). Model 6 proposed by [37] also considers $\varepsilon^{pred}_{eff} = 0.004$, and they think the shear strength provided by FRCM system can be calculated by summarizing the contribution of the textile and the associated mortar. Model 6 has an average $v^{exp}_{FRCM}/v^{pred}_{FRCM}$ ratio (μ) of 1.48, SD of 2.05 and COV 1.39. As seen in Fig. 10(c), in most of the cases the model underestimates the shear strength of the strengthened beams. Model 5 [54] was first used in the design of the FRP system based on the experimental response of U-wrapped beams. In case of the FRCM systems, the tensile stress distribution along the shear cracks in the FRCM reinforced material is uneven and locally high due to the brittle behaviour of the mortar-based composite material. Meanwhile, tensile stress may allow partial failure before the entire cement composite material fails. Consequently, the efficiency of FRCM jackets is lower than that of FRP jackets, and in Model 5 this is considered by introducing the "effectiveness coefficient" k_e which is taken equal to 0.5 [21,51]. Model 5 has an average $v^{exp}_{FRCM}/v^{pred}_{FRCM}$ ratio (μ) of 2.22, SD of 0.91 and COV of 0.41. From Fig. 10(b), it seems that Model 5 has a similar behaviour with Models 4 and 6.

Fig. 11 depicts the experimental value of the fibre effective strain, ε^{exp}_{eff}, versus the predicted value, ε^{pred}_{eff}, as well as the normalized experimental value of effective strain $\varepsilon^{exp}_{eff}/\varepsilon_{fu}$ versus $\rho_f E_f / f'^{2/3}_c$ for Models 4, 5, and 6. Fig. 11(d-f) suggests similar to Models 1 and 2 that, $\varepsilon^{exp}_{eff}/\varepsilon_{fu}$ decreases with the increase of $\rho_f E_{FRCM}/f'^{2/3}_c$. $\varepsilon^{exp}_{eff}/\varepsilon_{fu}$ is almost always greater than 0.25 and $\rho_f E_{FRCM}/f'^{2/3}_c$ is less than 0.05 for nearly all non-detachment failed beams. The high consistency of these models verifies that $\rho_f E_{FRCM}/f'^{2/3}_c$ has an influence on ε_{eff}, which is also affected by the failure mode of the beam. The strengthened beams with $\varepsilon^{exp}_{eff}/\varepsilon_{fu} > 1$ correspond to 8.4 %, 55.9 % and 22.0 % (5, 33 and 13 beams) in case of Models 4, 5, and 6. As discussed in section 3.1.1.1, ε^{exp}_{eff} is not measured but it is defined after implementing Models 4, 5, and 6 for $V^{exp}_{FRCM} (= V_{JAC}$ see Table A).

When v^{exp}_{FRCM} is less than 0.5, Figs. 10 and 11 highlight that Models 4, 5, and 6, which are based on the properties of the composite material, outperform Models 1, 2, and 3, which rely on fiber properties. This is particularly evident when the detachment failure occurs. However, when considering the entire range, Models 4, 5, and 6 do not exhibit a significant advantage over Models 1, 2, and 3 in terms of MAE and RMSE. Consequently, the existing models are unable to provide accurate predictions for the shear strength contribution of FRCM.

3.2. Analytical models for FRC jacketing systems

The total shear strength of fibre-reinforced-cement system strengthened RC beams (V_{shear}) comprises shear strength contributions from concrete (V_C), steel stirrups (V_S) and FRC jacket (V_{FRC}):

$$V_{shear} = V_C + V_s + V_{FRC} \tag{12}$$

V_{FRC} is calculated according to ACI [57], *fib* Model Code [58] and the Japan Society of Civil Engineers [59] design codes that are presented in Table 5. The same models were adopted by Yin et al. [56]. In case of Models 7 and 8, V_C is defined by Eqs. (5) and (6), respectively, whereas V_s is defined according to Eq. (7). For Model 8, V_c is given by [60]:

$$V_c = \beta_d \beta_p \beta_n f_{vcd} b_w d / \gamma_b \tag{13}$$

where $f_{vd,FRC} = 0.3 f^{2/3}_{c,FRC}/\gamma_c$ is the design average tensile strength perpendicular to diagonal cracks; $f_{vcd} = 0.2\sqrt{f_c}$; $\beta_d = \sqrt[4]{\frac{1000}{d}} \leq 1.5$; $\beta_p = \sqrt[3]{100\rho_{long}} \leq 1.5$; $\beta_n = 1$ for the member without axial compressive force.

The experimental and the predicted normalised shear stress of the FRC jacketing system, v^{exp}_{FRC} and v^{pred}_{FRC}, are calculated from:

$$v^{exp}_{FRC} = \frac{V^{exp}_{FRC}}{b_w d f'_c}; v^{pred}_{FRC} = \frac{V^{pred}_{FRC}}{b_w d f'_c} \tag{13}$$

where $V^{exp}_{FRC} (= V_{JAC}$ see Table A) is the experimental shear strength provided by FRC jackets; V^{pred}_{FRC} is predicted the shear strength provided by FRCM jacket which is calculated by Models 7–9.

In the case of the ECC-R jacketed beams (13 specimens), Models 7–9 (Table 5) cannot be used to assess this system [59,60]. Additionally, due to missing information the beams of studies [15,29,36] were not used. In total 39 beams were used to calculate μ, SD, COV of $v^{exp}_{FRC}/v^{pred}_{FRC}$, as well as

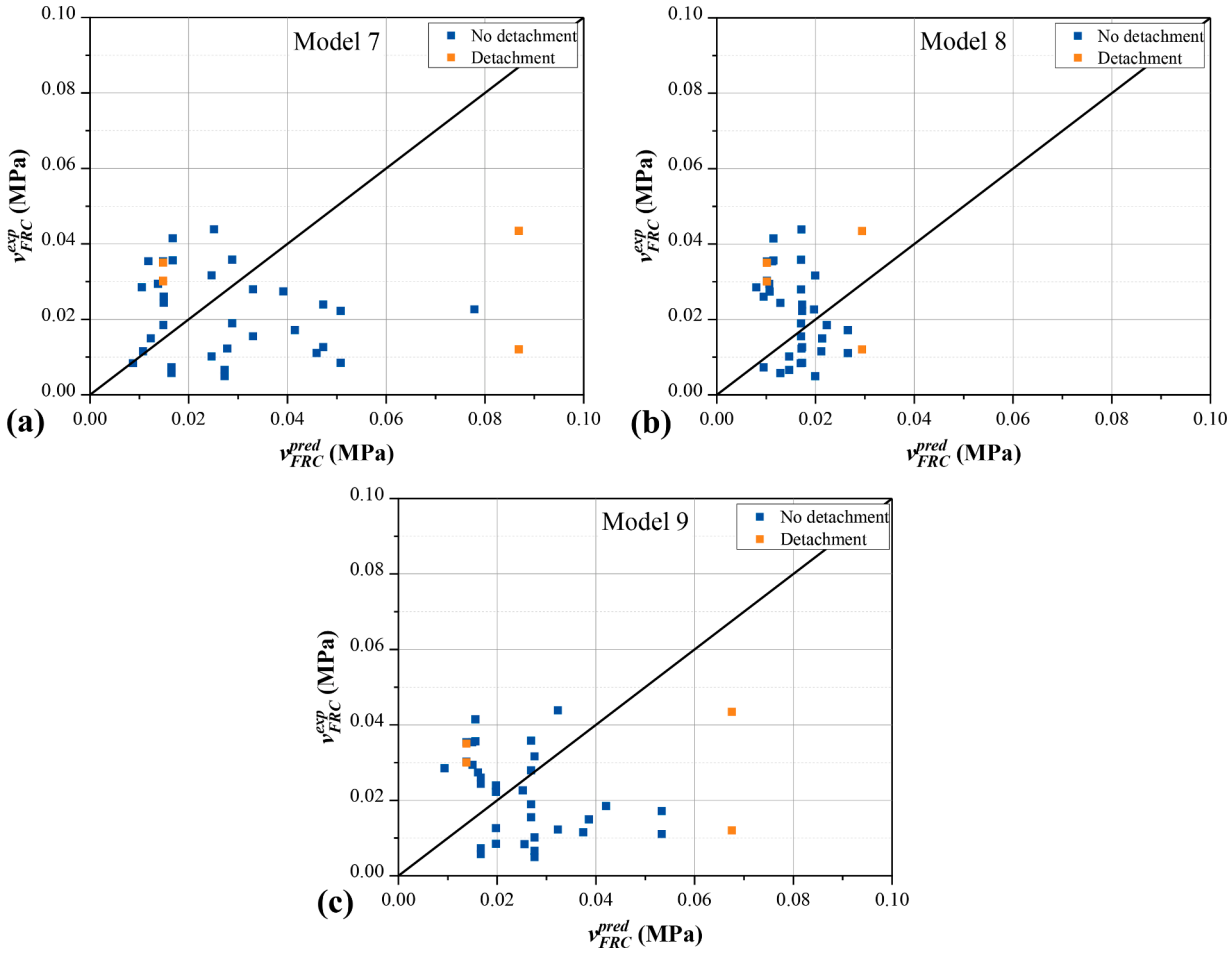

Fig. 12. Comparison between experimental, v_{FRC}^{exp} and predicted, v_{FRC}^{pred}, shear strength for: (a) Model 7; (b) Model 8; (c) Model 9.

MAE, RMSE of $v_{FRC}^{pred} - v_{FRC}^{exp}$ as presented in Table 6. Fig. 12 illustrates the relationship between v_{FRC}^{pred} and v_{FRC}^{exp} for Models 7–9.

Each of Models 7 [55], 8 [56] and 9 [57] rely on a different parameter to assess the shear strength contributed by the FRC system. Specifically, Model 7 considers the influence of the shear span ratio, Model 8 introduces the characteristic value of the final residual tensile strength of the FRC obtained by considering a crack opening equal to 1.5 mm, and Model 9 considers that the shear strength of the FRC comprises the shear strength of concrete and the shear strength of the fibres. Even though μ is larger than 1 in all models, still there is a certain number of beams where $v_{FRC}^{exp} < v_{FRC}^{pred}$ (Model 7: 20 beams, Model 8: 16 beams, Model 9: 18, Fig. 12). Models 7 and 9 seem to be equivalent. However, the dispersion is high in all models, leaving much room for the development of more reliable formulas for the various FRC strengthening systems.

4. Conclusions

This paper presents a review on the shear strengthening of existing RC beams with mortar-based composites. Experimental data from 36 studies were collected and an experimental database that comprises 218 RC beams was compiled. 164 beams were retrofitted using FRCM systems and 54 beams using alternative mortar-based composites. The impact of the design parameters of the beams and the mortar-based composite systems on the shear strength increase was thoroughly presented and discussed. The various failure modes of the strengthened beams were classified. Furthermore, existing design models proposed to predict the contribution of the mortar-based composites to the shear strength of RC beams were assessed using the database. The main conclusions drawn are the following:

- Experimental evidence has demonstrated that the strengthening effect of the externally applied mortar-based composites is higher when the concrete compressive strength $f_c^{'} < 30MPa$ and it reduces as the internal shear reinforcement (ρ_w) increases. It seems that the presence of the externally bonded system limits the strain of the internal shear links preventing them from reaching their yielding strength.
- Mortar-based composites is an effective system in increasing the shear capacity of deficient RC beams. When FRCM jacketing is applied, shear strength of RC beams increased from 4 % to 196 % (61 % on average), whereas in case of FRC systems from 4 % to 190 % (by 80 % on average).
- Carbon textiles are the most popular among the textiles used in FRCM (CFRCM) systems (>50 % of the beams were jacketed with carbon textiles) reaching a shear strength increase up to 196 %. For similar axial rigidity values, PFRCM systems are less effective. The average V_{JAC}/V_{CON} for the B-, C- G-, PFRCM and SRG jackets is 110 %, 86 %, 69 %, 25 %, and 62 %, respectively. SRG, C- and BFRCM exhibit similar shear strength enhancement capacity.
- U-shaped jacketing is the most popular configuration (74 % of the beams) with the failure mode observed being detachment of the jacket. In general, the alternative anchorage systems discussed herein effectively prevented detachment of the FRCM jacketing system, however near surface mounted (NSM) anchors seem to be less effective. In case of side bonded beams, the anchorage systems

Table A1
Database of mortar-based composite systems.

Ref.	Name	Beam details							Mortar-based system details												Test Results		
		Shape	b_w	d	a/d	f'_c	ρ_{long}	ρ_w	SC	TYPE	Anchors	t_{cf}	ε_{fu}	E_f	n	ρ_f*	t_{cm}	f'_{cm}	E_{frcm}	ρ_{cm}	FM	V_{JAC}	V_{JAC}/V_{CON}
			mm	mm		MPa	%	%						GPa			mm	MPa	GPa				kN	
[11]	BS1-L	R	180	334	3.1	34	2.6	0.00	U	S	–	0.084	0.0150	190	2	0.0019	12	50	NR	0.133	SH	73.1	0.87
	BS1-H	R	180	334	3.1	34	2.6	0.00	U	S	–	0.169	0.0150	190	2	0.0038	12	50	NR	0.133	SH	103.7	1.23
	BS-L	R	180	334	2.6	34	2.6	0.00	U	S	–	0.084	0.0150	190	2	0.0019	12	50	NR	0.133	SH	125.5	1.12
	BS-H	R	180	334	2.6	34	2.6	0.00	U	S	–	0.169	0.0150	190	2	0.0038	12	50	NR	0.133	SH	148.8	1.33
	BS3-L	R	180	334	2.1	34	2.6	0.00	U	S	–	0.084	0.0150	190	2	0.0019	12	50	NR	0.133	SH	122.9	0.66
	BS3-H	R	180	334	2.1	34	2.6	0.00	U	S	–	0.169	0.0150	190	2	0.0038	12	50	NR	0.133	SH	139.7	0.75
	BS4-L	R	180	334	1.6	34	2.6	0.00	U	S	–	0.084	0.0150	190	2	0.0019	12	50	NR	0.133	SH	59.0	0.20
	BS4-H	R	180	334	1.6	34	2.6	0.00	U	S	–	0.169	0.0150	190	2	0.0038	12	50	NR	0.133	SH	91.3	0.32
[18]	BGS	R	200	423	2.6	28.3	4.75	0.12	SB(T)	E-N-M	–	–	–	–	–	–	20	36.7	–	–	SH	13.50	0.04
[24]	S/d1.5S1	R	150	280	1.5	30.0	3.50	0.19	SB(T)	E-PE	–	–	–	–	–	0.02	10	128	–	–	SH	27.10	0.10
	S/d1.5S2	R	150	280	1.5	30.0	3.50	0.19	SB(T)	E-PE	–	–	–	–	–	0.02	10	128	–	–	SH	51.20	0.18
	S/d2.5S1	R	150	280	2.5	30.0	3.50	0.19	SB(T)	E-PE	–	–	–	–	–	0.02	10	128	–	–	SH	22.20	0.13
	S/d2.5S2	R	150	280	2.5	30.0	3.50	0.19	SB(T)	E-PE	–	–	–	–	–	0.02	10	128	–	–	SH	39.95	0.24
[25]	a-N-E-Cast	R	150	265	2.3	26.3	2.37	0.00	SB(T)	E-PE	–	–	–	–	–	0.02	20	25	–	–	SH	16.81	0.77
	b-B-E-Cast	R	150	265	2.3	26.3	2.37	0.00	SB(T)	E-PE-R	–	–	–	–	–	0.02	20	25	–	–	SH	19.13	0.88
	c-N-E-Cast	R	150	265	3.0	26.3	2.37	0.00	SB(T)	E-PE	–	–	–	–	–	0.02	20	25	–	–	SH	11.29	0.51
[26]	R 0.44-NS-F0	R	150	156	4.5	30.0	0.97	0.00	U	E-N	–	–	–	–	–	0.0	50	–	–	–	SH	4.00	0.15
	R 0.44-NS-F0.5	R	150	156	4.5	30.0	0.97	0.00	U	E-N	–	–	–	–	–	0.005	50	–	–	–	SH	5.00	0.19
	R 0.44-NS-F1.0	R	150	156	4.5	30.0	0.97	0.00	U	E-N	–	–	–	–	–	0.01	50	–	–	–	SH	11.50	0.44
	R 0.44-NS-F1.5	R	150	156	4.5	30.0	0.97	0.00	U	E-N	–	–	–	–	–	0.015	50	–	–	–	SH	31.50	1.21
[4]	AUH1	R	200	270	2.2	28	0.4	0.00	U	S	–	0.254	0.0150	190	1	0.0025	7	55	25	0.070	F	13.1	0.28
	AUML1	R	200	270	2.2	28	0.4	0.00	U	S	YES	0.084	0.0150	190	1	0.0008	7	55	25	0.070	F	16.3	0.34
	AFL1	R	200	270	2.2	28	0.4	0.00	F	S	–	0.084	0.0150	190	1	0.0008	7	55	25	0.070	F	18.1	0.38
	AFH1	R	200	270	2.2	28	0.4	0.00	F	S	–	0.254	0.0150	190	1	0.0025	7	55	25	0.070	F	13.6	0.29
	BUL1	R	200	270	2.2	23	1.5	0.00	U	S	–	0.084	0.0150	190	1	0.0008	7	55	25	0.070	SH	71.9	1.05
	BUL2	R	200	270	2.2	23	1.5	0.00	U	S	–	0.084	0.0150	190	2	0.0017	10	55	25	0.100	SH	68.3	1.00
	BUML1	R	200	270	2.2	23	1.5	0.00	U	S	YES	0.084	0.0150	190	1	0.0008	7	55	25	0.070	SH	77.7	1.14
	BFL1	R	200	270	2.2	23	1.5	0.00	F	S	–	0.084	0.0150	190	1	0.0008	7	55	25	0.070	F	77.5	1.13
	BFH1	R	200	270	2.2	23	1.5	0.00	F	S	–	0.084	0.0150	190	2	0.0017	10	55	25	0.100	F	109.1	1.60
[10]	B_P1	T	150	335	2.4	39	3.1	0.27	U	PBO	YES	0.046	0.0215	270	1	0.0003	8	30	NR	0.060	SH	17.9	0.09
	B_P2	T	150	335	2.4	39	3.1	0.27	U	PBO	YES	0.046	0.0215	270	1	0.0003	8	30	NR	0.060	SH	44.7	0.23
	B_P3	T	150	335	2.4	39	3.1	0.27	U	PBO	YES	0.046	0.0215	270	1	0.0003	8	30	NR	0.060	SH	33.7	0.17
	B_WS1	T	150	335	2.4	39	3.1	0.27	U	PBO	YES	0.046	0.0215	270	1	0.0003	8	30	NR	0.060	SH	38.1	0.19
	B_WS2	T	150	335	2.4	39	3.1	0.27	U	PBO	YES	0.046	0.0215	270	1	0.0003	8	30	NR	0.060	SH	41.5	0.21
	B_WS3	T	150	335	2.4	39	3.1	0.27	U	PBO	YES	0.046	0.0215	270	1	0.0003	8	30	NR	0.060	SH	37.8	0.19
	B_W1	T	150	335	2.4	39	3.1	0.27	U	PBO	YES	0.046	0.0215	270	1	0.0003	8	30	NR	0.060	SH	54.5	0.27
	B_W2	T	150	335	2.4	39	3.1	0.27	U	PBO	YES	0.046	0.0215	270	1	0.0003	8	30	NR	0.060	SH	39.1	0.20
	B_W3	T	150	335	2.4	39	3.1	0.27	U	PBO	YES	0.046	0.0215	270	1	0.0003	8	30	NR	0.060	SH	30.7	0.15
[12]	B1-U-L	T	180	335	2.8	34	4.1	0.00	U	S	–	0.084	0.0150	190	2	0.0019	12	50	20	0.133	SH	86.4	0.71
	B1-U-H	T	180	335	2.8	34	4.1	0.00	U	S	–	0.169	0.0150	190	2	0.0038	12	50	20	0.133	SH	79.2	0.65
	B1-S-L	T	180	335	2.8	34	4.1	0.00	SB	S	–	0.084	0.0150	190	2	0.0019	12	50	20	0.133	SH	60.8	0.50
	B1-S-H	T	180	335	2.8	34	4.1	0.00	SB	S	–	0.169	0.0150	190	2	0.0038	12	50	20	0.133	SH	51.2	0.42
	B2-U-L	T	180	335	2.8	34	4.1	0.10	U	S	–	0.084	0.0150	190	2	0.0019	12	50	20	0.133	SH	60.8	0.36
	B2-U-H	T	180	335	2.8	34	4.1	0.10	U	S	–	0.169	0.0150	190	2	0.0038	12	50	20	0.133	SH	43.5	0.26
	B3-U-L	T	180	335	2.8	34	4.1	0.21	U	S	–	0.084	0.0150	190	2	0.0019	12	50	20	0.133	SH	43.9	0.22
	B3-U-H	T	180	335	2.8	34	4.1	0.21	U	S	–	0.169	0.0150	190	2	0.0038	12	50	20	0.133	SH	19.7	0.10
[14]	0F-8D12	R	150	250	2.8	32.4	2.62	0.11	SB(T)	E-S	YES	–	–	–	–	0.0	10	56.8	–	–	SH	48.80	0.90
	1F-8D12	R	150	250	2.8	36.7	2.62	0.11	SB(T)	E-S	YES	–	–	–	–	1.0	10	69.7	–	–	SH	45.90	0.85
	1.5F-8D12	R	150	250	2.8	32.4	2.62	0.11	SB(T)	E-S	YES	–	–	–	–	1.5	10	60.8	–	–	SH	57.15	1.05
	1.5F-4D12	R	150	250	2.8	36.7	2.62	0.11	SB(T)	E-S	YES	–	–	–	–	1.5	10	60.8	–	–	SH	55.30	1.02
	1.5F-6D12	R	150	250	2.8	36.7	2.62	0.11	SB(T)	E-S	YES	–	–	–	–	1.5	10	60.8	–	–	SH	47.20	0.87

(*continued on next page*)

Table A1 (*continued*)

Ref.	Name	Beam details							Mortar-based system details											Test Results		
		Shape	b_w	d	a/d	f'_c	ρ_{long}	ρ_w	SC	TYPE	Anchors	t_{cf}	ε_{fu}	E_f	n	ρ_f*	t_{cm}	f'_{cm}	E_{frcm}	ρ_{cm}	FM	V_{JAC}	V_{JAC}/V_{CON}
			mm	mm		MPa	%	%						GPa			mm	MPa	GPa			kN	
	1.5F-6D10	R	150	250	2.8	36.7	2.62	0.11	SB(T)	E-S	YES	–	–	–	–	1.5	10	60.8	–	–	SH	46.90	0.87
	1.5F-8D10	R	150	250	2.8	36.7	2.62	0.11	SB(T)	E-S	YES	–	–	–	–	1.5	10	60.8	–	–	SH	54.70	1.01
[15]	EJ-UR	R	150	124	1.6	28.6	1.22	0.89	U	E-S	–	–	–	–	–	2.0	50	118	–	–	SH	−3.63	–
	EJ-O/R	R	150	124	1.6	28.6	2.16	0.89	SB(T)	E-S	–	–	–	–	–	2.0	50	118	–	–	SH	−1.26	–
[16]	SA-20–2	R	150	257	2.0	44.8	1.04	0.00	SB(T)	E-PVA	–	–	–	–	–	1.5	20	44.8	–	–	SH	57.00	0.84
	SA-20–3	R	150	257	3.0	44.8	1.04	0.00	SB(T)	E-PVA	–	–	–	–	–	1.5	20	44.8	–	–	SH	16.00	0.38
	SB-20–2	R	150	252.5	2.0	44.8	2.59	0.00	SB(T)	E-PVA	–	–	–	–	–	1.5	20	44.8	–	–	SH	52.50	0.57
	SB-20–3	R	150	252.5	3.0	44.8	2.59	0.00	SB(T)	E-PVA	–	–	–	–	–	1.5	20	44.8	–	–	SH	12.50	0.20
	SA-40–2	R	150	257	2.0	44.8	1.04	0.00	SB(T)	E-PVA	–	–	–	–	–	1.5	40	44.8	–	–	SH	27.00	0.40
	SA-40–3	R	150	257	3.0	44.8	1.04	0.00	SB(T)	E-PVA	–	–	–	–	–	1.5	40	44.8	–	–	SH	17.50	0.41
	SB-40–2	R	150	252.5	2.0	44.8	2.59	0.00	SB(T)	E-PVA	–	–	–	–	–	1.5	40	44.8	–	–	SH	82.50	0.89
	SB-40–3	R	150	252.5	3.0	44.8	2.59	0.00	SB(T)	E-PVA	–	–	–	–	–	1.5	40	44.8	–	–	SH	13.00	0.21
[20]	E-C-A	R	150	280	2	25.8	1.4	0.18	SB	C	–	0.047	0.018	240	3	0.0012	20	20	NR	0.175	SH	36.9	0.40
	E-G-A	R	150	280	2	25.8	1.4	0.18	SB	G	–	0.047	0.0325	80	3	0.0012	20	40	NR	0.175	SH	20.0	0.22
	E-P-A	R	150	280	2	25.8	1.4	0.18	SB	PBO	–	0.046	0.0215	270	3	0.0012	20	30	NR	0.175	SH	23.4	0.25
	E-C-UA	R	150	280	2	25.8	1.4	0.18	SB	C	–	0.047	0.018	240	3	0.0012	20	20	NR	0.175	SH	35.5	0.36
	E-G-UA	R	150	280	2	25.8	1.4	0.18	SB	G	–	0.047	0.0325	80	3	0.0012	20	40	NR	0.175	SH	16.3	0.17
	E-P-UA	R	150	280	2	25.8	1.4	0.18	SB	PBO	–	0.046	0.0215	270	3	0.0012	20	30	NR	0.175	SH	26.3	0.27
[27]	Bi10-GM1-A	R	150	270	2.6	34	2.8	0.13	U	C	YES	0.110	0.0180	242	1	0.0015	6	43.4	NR	0.080	SH	57.5	0.68
	Bi10-GM1	R	150	270	2.6	34	2.8	0.13	U	C	–	0.110	0.0180	242	1	0.0015	6	43.4	NR	0.080	SH	40.0	0.47
	Bi7-GM1-A	R	150	270	2.6	34	2.8	0.13	U	C	YES	0.110	0.0180	242	1	0.0015	6	43.4	NR	0.080	SH	72.5	0.85
	Bi7-GM1	R	150	270	2.6	34	2.8	0.13	U	C	–	0.110	0.0180	242	1	0.0015	6	43.4	NR	0.080	SH	60.0	0.71
	Bi10-GM2-A	R	150	270	2.6	34	2.8	0.13	U	C	YES	0.110	0.0180	242	2	0.0029	9	43.4	NR	0.120	SH	107.5	1.26
	Bi10-GM2	R	150	270	2.6	34	2.8	0.13	U	C	–	0.110	0.0180	242	2	0.0029	9	43.4	NR	0.120	SH	90.0	1.06
	Bi10-GM3	R	150	270	2.6	34	2.8	0.13	U	C	–	0.110	0.0180	242	3	0.0044	12	43.4	NR	0.160	SH	30.0	0.35
	Uni10-GM1	R	150	270	2.6	34	2.8	0.13	U	C	–	0.110	0.0180	242	1	0.0015	6	43.4	NR	0.080	SH	95.0	1.12
[28]	S-20–2	R	150	257	2.0	26.6	0.82	0.00	SB(T)	E-N	–	–	–	–	–	–	20	56	–	–	SH	57.00	0.84
	S-20–3	R	150	257	3.0	26.6	0.82	0.00	SB(T)	E-N	–	–	–	–	–	–	20	56	–	–	SH	16.00	0.38
	S-40–2	R	150	257	2.0	26.6	0.68	0.00	SB(T)	E-N	–	–	–	–	–	–	40	56	–	–	SH	27.00	0.40
	S-40–3	R	150	257	3.0	26.6	0.68	0.00	SB(T)	E-N	–	–	–	–	–	–	40	56	–	–	SH	17.50	0.41
[29]	ST-1S-R	R	150	250	2.1	30.0	1.36	0.13	SB	E-S	YES	–	–	–	–	2.0	60	135.4	–	–	F	108.00	1.88
	ST-2S-R	R	150	250	2.1	30.0	1.36	0.13	SB(T)	E-S	YES	–	–	–	–	2.0	30	135.4	–	–	S	68.5	1.19
[30]	B_P100_BZ	T	150	335	2.4	36	3.1	0.27	U	PBO	–	0.046	0.0215	270	1	0.0003	8	30	NR	0.053	SH	11.9	0.05
	B_P100_1	T	150	335	2.4	36	3.1	0.27	U	PBO	YES	0.046	0.0215	270	1	0.0003	8	30	NR	0.053	SH	27.3	0.12
	B_P100_2	T	150	335	2.4	36	3.1	0.27	U	PBO	YES	0.046	0.0215	270	1	0.0003	8	30	NR	0.053	SH	22.9	0.10
	B_P100_3	T	150	335	2.4	36	3.1	0.27	U	PBO	YES	0.046	0.0215	270	1	0.0003	8	30	NR	0.053	SH	22.8	0.10
[31]	B1	T	150	335	2.4	39	3.1	0.27	U	PBO	YES	0.046	0.0215	270	1	0.0003	8	30	NR	0.048	SH	36.9	0.16
[9]	S0-CM	R	250	317	3.2	61	3.7	0.00	SB	C	–	0.128	0.0160	230	1	NR	8	58	21	0.064	SH	125.6	0.87
	S50-CM	R	250	317	3.2	61	3.7	0.11	SB	C	–	0.128	0.0160	230	1	NR	8	58	21	0.064	SH	79.2	0.30
	S150-CM	R	250	317	3.2	61	3.7	0.19	SB	C	–	0.128	0.0160	230	1	NR	8	58	21	0.064	SH	78.5	0.26
[32]	CL1	R	102	177	2.6	20	2.2	0.00	U	C	–	0.062	0.0079	225	1	0.0012	4	38.7	NR	0.078	SH	28.9	0.97
	CL1_strips	R	102	177	2.6	17	2.2	0.00	U	C	–	0.062	0.0079	225	2	0.0009	6	38.7	NR	0.090	SH	33.7	1.13
	CH1	R	102	177	2.6	20	2.2	0.00	U	C	–	0.095	0.0079	225	1	0.0019	4	31.1	NR	0.078	SH	15.1	0.51
	CH1_CL1	R	102	177	2.6	17	2.2	0.00	U	C	–	0.079	0.0079	225	2	0.0031	6	38.7	NR	0.118	SH	37.6	1.27
	CH2	R	102	177	2.6	20	2.2	0.00	U	C	–	0.095	0.0079	225	2	0.0037	6	31.1	NR	0.118	SH	39.2	1.32
	CL3	R	102	177	2.6	18	2.2	0.00	U	C	–	0.062	0.0079	225	3	0.0036	8	35.5	NR	0.157	SH	37.9	1.28
	CH2_CH1	R	102	177	2.6	17	2.2	0.00	U	C	–	0.079	0.0079	225	3	0.0049	8	38.7	NR	0.157	SH	44.4	1.49
	CH3	R	102	177	2.6	19	2.2	0.00	U	C	–	0.095	0.0079	225	3	0.0056	8	26.9	NR	0.157	SH	45.4	1.53
	CH3_CL1	R	102	177	2.6	17	2.2	0.00	U	C	–	0.079	0.0079	225	4	0.0068	10	38.7	NR	0.196	SH	48.5	1.63
	G1	R	102	177	2.6	17	2.2	0.00	U	G	–	0.044	0.0166	74	1	0.0009	4	35.5	NR	0.078	SH	12.2	0.41
	G3	R	102	177	2.6	17	2.2	0.00	U	G	–	0.044	0.0166	74	3	0.0026	8	35.5	NR	0.157	SH	37.0	1.25
	G7	R	102	177	2.6	17	2.2	0.00	U	G	–	0.044	0.0166	74	7	0.0060	16	38.7	NR	0.314	SH	53.0	1.78

(*continued on next page*)

Table A1 (*continued*)

Ref.	Name	Beam details							Mortar-based system details											Test Results		
		Shape	b_w	d	a/d	f'_c	ρ_{long}	ρ_w	SC	TYPE	Anchors	t_{cf}	ε_{fu}	E_f	n	ρ_f*	t_{cm}	f'_{cm}	E_{frcm}	ρ_{cm}	FM	V_{JAC}	V_{JAC}/V_{CON}
			mm	mm		MPa	%	%						GPa			mm	MPa	GPa			kN	
	B1	R	102	177	2.6	20	2.2	0.00	U	B	–	0.037	0.0183	89	1	0.0007	4	33.3	NR	0.078	SH	14.4	0.48
	B3	R	102	177	2.6	20	2.2	0.00	U	B	–	0.037	0.0183	89	3	0.0022	8	35.5	NR	0.157	SH	36.1	1.22
	B7	R	102	177	2.6	20	2.2	0.00	U	B	–	0.037	0.0183	89	7	0.0051	16	35.5	NR	0.314	SH	47.9	1.61
	CL1_1.6	R	102	177	1.6	19	2.2	0.00	U	C	–	0.062	0.0079	225	1	0.0012	4	33.3	NR	0.078	SH	26.1	0.40
	CL3_1.6	R	102	177	1.6	19	2.2	0.00	U	C	–	0.062	0.0079	225	3	0.0036	8	33.3	NR	0.157	SH	40.2	0.61
	CL1_3.6	R	102	177	3.6	19	2.2	0.00	U	C	–	0.062	0.0079	225	1	0.0012	4	33.3	NR	0.078	SH	29.4	1.15
	CL3_3.6	R	102	177	3.6	19	2.2	0.00	U	C	–	0.062	0.0079	225	3	0.0036	8	33.3	NR	0.157	SH	39.6	1.55
[33]	C0	R	150	280	2.0	30	1.4	0.00	U	C	–	0.047	0.0180	240	2	0.0013	9	20	NR	0.120	SH	56.8	0.77
	P0	R	150	280	2.0	30	1.4	0.00	U	PBO	–	0.045	0.0215	270	2	0.0012	12	40	NR	0.160	SH	46.2	0.63
	G0	R	150	280	2.0	30	1.4	0.00	U	G	–	0.047	0.0325	80	2	0.0013	15	22	NR	0.200	SH	49.7	0.67
	C1	R	150	280	2.0	30	1.4	0.18	U	C	–	0.047	0.0180	240	2	0.0013	9	20	NR	0.120	SH	46.9	0.47
	P1	R	150	280	2.0	30	1.4	0.18	U	PBO	–	0.045	0.0215	270	2	0.0012	12	40	NR	0.160	SH	29.1	0.29
	G1	R	150	280	2.0	30	1.4	0.18	U	G	–	0.047	0.0325	80	2	0.0013	15	22	NR	0.200	SH	38.3	0.38
[34]	C_Full	R	150	296	1.8	30	1.3	0.00	U	C	–	0.047	0.0180	240	2	0.0013	13	20	NR	0.173	F	75.3	1.02
	C_Intermittent	R	150	296	1.8	30	1.3	0.00	U	C	–	0.047	0.0180	240	2	0.0008	13	20	NR	0.114	SH	52.6	0.71
	P_Full	R	150	296	1.8	30	1.3	0.00	U	PBO	–	0.045	0.0215	270	2	0.0012	13	30	NR	0.173	SH	33.4	0.45
	P_Intermittent	R	150	296	1.8	30	1.3	0.00	U	PBO	–	0.045	0.0215	270	2	0.0008	13	30	NR	0.114	SH	24.2	0.33
	G_Full	R	150	296	1.8	30	1.3	0.00	U	G	–	0.047	0.0325	80	2	0.0013	13	40	NR	0.173	SH	45.5	0.62
	G_Intermittent	R	150	296	1.8	30	1.3	0.00	U	G	–	0.047	0.0325	80	2	0.0008	13	40	NR	0.114	SH	23.4	0.32
[35]	S0-CM	R	250	311	1.6	61	3.8	0.00	SB	C	–	0.128	0.0160	234.5	1	NR	8	58	NR	0.064	SH	136.5	0.23
	S50-CM	R	250	311	1.6	61	3.8	0.09	SB	C	–	0.128	0.0160	234.5	1	NR	8	58	NR	0.064	SH	106.3	0.16
[36]	ST-1S	R	150	250	2.1	30.0	1.36	0.13	SB	E-S	–	–	–	–	–	2.0	30	135.4	–	–	SH	19.00	0.33
	ST-2S	R	150	250	2.1	30.0	1.36	0.13	SB(T)	E-S	–	–	–	–	–	2.0	60	135.4	–	–	F	83.00	1.44
[13]	B	R	150	267	2.2	35.0	2.35	0.33	SB	E-N	–	–	–	–	–	–	20	72.60	–	–	SH	43.60	1.00
	C	R	150	267	2.2	35.0	2.35	0.33	SB	E-N	–	–	–	–	–	–	20	30.20	–	–	SH	45.34	1.04
	D	R	150	267	2.2	35.0	2.35	0.33	SB	E-N-R	–	–	–	–	–	–	20	30.20	–	–	SH	54.06	1.24
[23]	S1-FRCM-F3-UA	R	150	230	3.3	23	6.1	0.23	U	C	YES	0.047	0.0180	240	1	0.0006	8	45.2	NR	0.107	SH	29.9	0.26
	S1-FRCM-F4-UN	R	150	230	3.3	21	6.1	0.23	U	S	–	0.047	0.0160	190	1	0.0006	8	45.2	NR	0.107	SH	34.5	0.30
	S1-FRCM-F4-UA	R	150	230	3.3	21	6.1	0.23	U	S	YES	0.047	0.0160	190	1	0.0006	8	45.2	NR	0.107	SH	34.9	0.30
	S-FRCM-F3-UN	R	150	230	3.3	25	6.1	0.33	U	C	–	0.270	0.0180	240	1	0.0036	8	45.2	NR	0.107	SH	24.3	0.19
	S-FRCM-F4-UN	R	150	230	3.3	21	6.1	0.33	U	S	–	0.270	0.0160	190	1	0.0036	8	45.2	NR	0.107	SH	17.5	0.13
	S-FRCM-F4-UA	R	150	230	3.3	21	6.1	0.33	U	S	YES	0.270	0.0160	190	1	0.0036	8	45.2	NR	0.107	SH	31.3	0.24
[37]	C–F–90	R	150	280	2.0	30	1.4	0.00	SB	C	–	0.047	0.0180	240	2	0.0013	12	20	NR	0.160	SH	75.1	1.02
	C–I–90	R	150	280	2.0	30	1.4	0.00	SB	C	–	0.047	0.0180	240	2	0.0008	12	20	NR	0.105	SH	52.3	0.71
	C–I–45	R	150	280	2.0	30	1.4	0.00	SB	C	–	0.047	0.0180	240	2	0.0007	12	20	NR	0.083	SH	33.7	0.46
	C–I–90–A	R	150	280	2.0	30	1.4	0.00	SB	C	YES	0.047	0.0180	240	2	0.0008	12	20	NR	0.105	SH	54.1	0.73
	C–I–45–A	R	150	280	2.0	30	1.4	0.00	SB	C	YES	0.047	0.0180	240	2	0.0007	12	20	NR	0.083	SH	36.3	0.49
	P–F–90	R	150	280	2.0	30	1.4	0.00	SB	PBO	–	0.045	0.0215	270	2	0.0012	12	30	NR	0.160	SH	33.6	0.45
	P–I–90	R	150	280	2.0	30	1.4	0.00	SB	PBO	–	0.045	0.0215	270	2	0.0008	12	30	NR	0.105	SH	23.9	0.32
	P–I–45	R	150	280	2.0	30	1.4	0.00	SB	PBO	–	0.045	0.0215	270	2	0.0006	12	30	NR	0.083	SH	39.3	0.53
	P–I–90–A	R	150	280	2.0	30	1.4	0.00	SB	PBO	YES	0.045	0.0215	270	2	0.0008	12	30	NR	0.105	SH	25.4	0.34
	P–I–45–A	R	150	280	2.0	30	1.4	0.00	SB	PBO	YES	0.045	0.0215	270	2	0.0006	12	30	NR	0.083	SH	40.5	0.55
	G–F–90	R	150	280	2.0	30	1.4	0.00	SB	G	–	0.047	0.0325	80	2	0.0013	12	40	NR	0.160	SH	45.4	0.61
	G–I–90	R	150	280	2.0	30	1.4	0.00	SB	G	–	0.047	0.0325	80	2	0.0008	12	40	NR	0.105	SH	23.4	0.32
	G–I–45	R	150	280	2.0	30	1.4	0.00	SB	G	–	0.047	0.0325	80	2	0.0007	12	40	NR	0.083	SH	−7.1	−9.60
	G–I–90–A	R	150	280	2.0	30	1.4	0.00	SB	G	YES	0.047	0.0325	80	2	0.0008	12	40	NR	0.105	SH	30.5	0.41
	G–I–45–A	R	150	280	2.0	30	1.4	0.00	SB	G	YES	0.047	0.0325	80	2	0.0007	12	40	NR	0.083	SH	12.8	0.17
[38]	BA-S-1	R	203	275	2.5	45	12.0	0.61	U	PBO	–	0.050	0.0120	270	1	0.0002	6	38	NR	0.030	SH	29.5	0.18
	BA-S-4	R	203	275	2.5	45	12.0	0.61	U	PBO	–	0.050	0.0120	270	4	0.0010	15	38	NR	0.074	SH	29.5	0.18
	BA-C-4	R	203	275	2.5	45	12.0	0.61	U	PBO	–	0.050	0.0120	270	4	0.0020	15	38	NR	0.148	SH	51.0	0.31
	BB-S-1	R	203	275	2.5	45	12.0	0.00	U	PBO	–	0.050	0.0120	270	1	0.0002	6	38	NR	0.030	SH	−12.5	−0.11
	BB-S-4	R	203	275	2.5	45	12.0	0.00	U	PBO	–	0.050	0.0120	270	4	0.0010	15	38	NR	0.074	SH	4.0	0.04

(*continued on next page*)

Table A1 (*continued*)

Ref.	Name	Beam details							Mortar-based system details											Test Results		
		Shape	b_w	d	a/d	f'_c	ρ_{long}	ρ_w	SC	TYPE	Anchors	t_{cf}	ε_{fu}	E_f	n	ρ_f*	t_{cm}	f'_{cm}	E_{frcm}	ρ_{cm}	FM	V_{JAC}	V_{JAC}/V_{CON}
			mm	mm		MPa	%	%						GPa			mm	MPa	GPa			kN	
	BB-C-1	R	203	275	2.5	45	12.0	0.00	U	PBO	–	0.050	0.0120	270	1	0.0005	6	38	NR	0.059	SH	23.5	0.21
[8]	CH2	T	200	385	2.3	18	3.2	0.00	U	C	–	0.950	0.0079	225	2	0.0190	6	37.4	NR	0.060	SH	47.0	0.38
	CL3	T	200	385	2.3	16	3.2	0.00	U	C	–	0.620	0.0079	225	3	0.0186	8	35.8	NR	0.080	SH	57.6	0.47
	CH4	T	200	385	2.3	16	3.2	0.00	U	C	–	0.950	0.0079	225	4	0.0380	10	36.1	NR	0.100	SH	96.5	0.78
	G7	T	200	385	2.3	18	3.2	0.00	U	G	–	0.440	0.0166	74	7	0.0308	16	33.7	NR	0.160	SH	94.2	0.77
	CH2_A100	T	200	385	2.3	17	3.2	0.00	U	C	YES	0.950	0.0079	225	2	0.0190	6	34.5	NR	0.060	SH	112.5	0.91
	CL3_A100	T	200	385	2.3	17	3.2	0.00	U	C	YES	0.620	0.0079	225	3	0.0186	8	37.9	NR	0.080	SH	114.0	0.93
	CH4_A50	T	200	385	2.3	17	3.2	0.00	U	C	YES	0.950	0.0079	225	4	0.0380	10	36.6	NR	0.100	SH	147.6	1.20
	CH4_A100	T	200	385	2.3	17	3.2	0.00	U	C	YES	0.950	0.0079	225	4	0.0380	10	33.4	NR	0.100	SH	237.5	1.93
	G7_A100	T	200	385	2.3	17	3.2	0.00	U	G	YES	0.440	0.0166	74	7	0.0308	16	37.4	NR	0.160	SH	107.2	0.87
[17]	B-E	R	250	300	3.3	24.4	0.99	0.21	U	E-PVA	–	–	–	–	–	–	40	63.2	–	–	SH	13.50	0.10
	B-M−6	R	250	300	3.3	25.2	0.99	0.21	U	E-PVA-R	–	–	–	–	–	–	40	28.1	–	–	SH	21.00	0.16
	B-M−1	R	250	300	3.3	25.0	0.99	0.21	U	E-PVA-R	–	–	–	–	–	–	40	62	–	–	SH	45.90	0.35
	B-E-6	R	250	300	3.3	24.5	0.99	0.21	U	E-PVA-R	–	–	–	–	–	–	40	49.6	–	–	SH	28.00	0.21
	B-E-1	R	250	300	3.3	24.9	0.99	0.21	U	E-PVA-R	–	–	–	–	–	–	40	53.4	–	–	SH	36.90	0.28
[39]	S0- FRCM-1	R	150	250	3.0	36	5.0	0.00	SB	C	–	1.000	0.0160	230	1	0.0133	12	74	22	0.160	SH	66.5	1.10
	S0- FRCM-2	R	150	250	3.0	36	5.0	0.00	SB	C	–	1.000	0.0160	230	2	0.0267	18	74	22	0.240	SH	87.2	1.45
	S1- FRCM-1	R	150	250	3.0	36	5.0	0.25	SB	C	–	1.000	0.0160	230	1	0.0133	12	74	22	0.160	SH	68.4	0.64
	S1- FRCM-2	R	150	250	3.0	36	5.0	0.25	SB	C	–	1.000	0.0160	230	2	0.0267	18	74	22	0.240	SH	72.1	0.67
	S- FRCM-1	R	150	250	3.0	36	5.0	0.50	SB	C	–	1.000	0.0160	230	1	0.0133	12	74	22	0.160	SH	67.6	0.51
	S- FRCM-2	R	150	250	3.0	36	5.0	0.50	SB	C	–	1.000	0.0160	230	2	0.0267	18	74	22	0.240	SH	73.6	0.55
[40]	SB_MCH2_20	R	102	177	2.6	19	2.2	0.00	SB	C	–	0.095	0.0079	225	2	0.0037	6	28.2	NR	0.118	SH	21.0	0.70
	SB_MCH2_150	R	102	177	2.6	19	2.2	0.00	SB	C	–	0.095	0.0079	225	2	0.0037	6	16.2	NR	0.118	SH	11.0	0.37
	SB_MCH3_20	R	102	177	2.6	19	2.2	0.00	SB	C	–	0.095	0.0079	225	3	0.0056	8	26.9	NR	0.157	SH	33.0	1.11
	SB_MCH3_150	R	102	177	2.6	19	2.2	0.00	SB	C	–	0.095	0.0079	225	3	0.0056	8	16.2	NR	0.157	SH	17.0	0.57
	UW_MCH2_20	R	102	177	2.6	20	2.2	0.00	U	C	–	0.095	0.0079	225	2	0.0037	6	31.1	NR	0.118	SH	39.0	1.31
	UW_MCH2_150	R	102	177	2.6	19	2.2	0.00	U	C	–	0.095	0.0079	225	2	0.0037	6	16.2	NR	0.118	SH	20.0	0.67
	UW_MCH3_20	R	102	177	2.6	19	2.2	0.00	U	C	–	0.095	0.0079	225	3	0.0056	8	26.9	NR	0.157	SH	45.0	1.51
	UW_MCH3_150	R	102	177	2.6	19	2.2	0.00	U	C	–	0.095	0.0079	225	3	0.0056	8	16.2	NR	0.157	SH	25.0	0.84
	UW_MCH3_100	R	102	177	2.6	18	2.2	0.00	U	C	–	0.095	0.0079	225	3	0.0056	8	17.3	NR	0.157	SH	45.0	1.51
	UW_MCH3_250	R	102	177	2.6	18	2.2	0.00	U	C	–	0.095	0.0079	225	3	0.0056	8	17	NR	0.157	SH	29.0	0.97
	UW_MCL3_20	R	102	177	2.6	18	2.2	0.00	U	C	–	0.062	0.0079	225	3	0.0036	8	38.7	NR	0.157	SH	38.0	1.28
	UW_MCL3_150	R	102	177	2.6	18	2.2	0.00	U	C	–	0.062	0.0079	225	3	0.0036	8	16.2	NR	0.157	SH	25.0	0.84
	UW_MG7_20	R	102	177	2.6	17	2.2	0.00	U	G	–	0.044	0.0166	74	7	0.0060	16	35.5	NR	0.314	SH	53.0	1.78
	UW_MG7_150	R	102	177	2.6	18	2.2	0.00	U	G	–	0.044	0.0166	74	7	0.0060	16	16.2	NR	0.314	SH	27.0	0.91
	FW_MCH2_20	R	102	177	2.6	19	2.2	0.00	F	C	–	0.095	0.0079	225	2	0.0037	6	28.2	NR	0.118	F	58.0	1.95
	FW_MCH2_150	R	102	177	2.6	19	2.2	0.00	F	C	–	0.095	0.0079	225	2	0.0037	6	16.2	NR	0.118	SH	48.0	1.61
	CH4_20	T	200	385	2.3	12	3.2	0.00	U	C	–	0.095	0.0079	225	4	0.0038	10	36.1	NR	0.100	SH	95.0	0.76
	CH4_150	T	200	385	2.3	12	3.2	0.00	U	C	–	0.095	0.0079	225	4	0.0038	10	22.9	NR	0.100	SH	66.0	0.53
	CH4_A100_20	T	200	385	2.3	11	3.2	0.00	U	C	Yes	0.095	0.0079	225	4	0.0038	10	33.4	NR	0.100	SH	236.0	1.90
	CH4_A100_150	T	200	385	2.3	12	3.2	0.00	U	C	Yes	0.095	0.0079	225	4	0.0038	10	19.3	NR	0.100	SH	119.0	0.96
[41]	L1	T	150	320	2.5	18	1.6	0.00	U	C	–	0.048	0.0180	225	1	0.0006	4	21.8	NR	0.053	SH	10.6	0.18
	L2	T	150	320	2.5	19	1.6	0.00	U	C	–	0.048	0.0180	225	2	0.0013	6	21.8	NR	0.080	SH	13.4	0.24
	H1	T	150	320	2.5	20	1.6	0.00	U	C	–	0.096	0.0180	225	1	0.0013	4	21.8	NR	0.053	SH	24.2	0.42
	H2	T	150	320	2.5	20	1.6	0.00	U	C	–	0.096	0.0180	225	2	0.0026	6	21.8	NR	0.080	SH	37.1	0.65
	L2A15ha	T	150	320	2.5	20	1.6	0.00	U	C	YES	0.048	0.0180	225	2	0.0013	6	21.8	NR	0.080	SH	59.7	1.04
	L2A10	T	150	320	2.5	11	1.6	0.00	U	C	YES	0.048	0.0180	225	2	0.0013	6	21.8	NR	0.080	SH	85.7	1.96
	H1A15	T	150	320	2.5	12	1.6	0.00	U	C	YES	0.096	0.0180	225	1	0.0013	4	21.8	NR	0.053	SH	54.7	1.25
	H2A10	T	150	320	2.5	12	1.6	0.00	U	C	YES	0.096	0.0180	225	2	0.0026	6	21.8	NR	0.080	SH	51.6	1.18
	H2A10	T	150	320	2.5	12	1.6	0.00	U	C	YES	0.096	0.0180	225	2	0.0026	6	21.8	NR	0.080	SH	52.1	0.91
[1]	SB-CT1	R	150	300	3.3	38	2.2	0.00	SB	C	–	0.128	0.0160	230	1	NR	7	58	NR	0.093	SH	16.0	0.26
	UW-CT1	R	150	300	3.3	38	2.2	0.00	U	C	–	0.128	0.0160	230	1	NR	7	58	NR	0.093	SH	14.1	0.23

(*continued on next page*)

Table A1 (*continued*)

Ref.	Name	Beam details						Mortar-based system details										Test Results		
		Shape	b_w	d	a/d	f'_c	ρ_{long}	ρ_w	SC	TYPE	Anchors	t_{cf}	ε_{fu}	E_f	n	ρ_f*	t_{cm}	f'_{cm}	E_{frcm}	ρ_{cm}	FM	V_{JAC}	V_{JAC}/V_{CON}
			mm	mm		MPa	%	%						GPa			mm	MPa	GPa				kN	
	SB-CT2	R	150	300	3.3	38	2.2	0.00	SB	C	–	0.128	0.0160	230	1	NR	7	58	NR	0.093	SH	60.9	0.99
	UW-CT2	R	150	300	3.3	38	2.2	0.00	U	C	–	0.128	0.0160	230	1	NR	7	58	NR	0.093	SH	64.9	1.05
[42]	1	R	150	231	1.7	26.3	1.74	0.30	U	E-S	–	–	–	–	–	–	30	26.3	–	–	SH	64.65	1.11
	2	R	150	231	1.7	26.3	1.74	0.30	U	E-S	–	–	–	–	–	–	30	26.3	–	–	SH	84.40	1.45
	3	R	150	231	1.7	26.3	1.74	0.00	U	E-S	–	–	–	–	–	–	30	26.3	–	–	SH	28.40	0.49
	7	R	150	231	1.7	26.3	1.74	0.30	U	E-S	–	–	–	–	–	–	30	85.7	–	–	SH	81.20	1.40
	8	R	150	231	1.7	26.3	1.74	0.30	U	E-S	–	–	–	–	–	–	30	85.7	–	–	SH	80.05	1.38
	9	R	150	231	1.7	26.3	1.74	0.00	U	E-S	–	–	–	–	–	–	30	85.7	–	–	SH	18.30	0.32
	13	R	150	231	1.7	26.3	1.74	0.30	U	E-S	–	–	–	–	–	–	30	95.3	–	–	SH	73.15	1.26
	14	R	150	231	1.7	26.3	1.74	0.30	U	E-S	–	–	–	–	–	–	30	95.3	–	–	SH	90.95	1.57
	15	R	150	231	1.7	26.3	1.74	0.00	U	E-S	–					–	30	95.3	–	–	SH	67.95	1.17

Note: 1. 'SC' is jacket's strengthening configuration: 'U' – U wrapped, 'F' – Fully wrapped, 'SB' – Side bonding (one side), 'SB(T)' – Side bonding (two sides).
Type: 'B' – BFRCM, 'C' – CFRCM, 'G' – GFRCM, 'PBO' – PBOFRCM, 'S' – SRG, 'E-N' – FRC (unknown fibre) without mesh/grid, 'E-N-R' – FRC (unknown fibre) with mesh/grid, 'E-PE' – FRC (PE fibre) without mesh/grid, 'E-PE-R' – FRC (PE fibre) with mesh/grid, 'E-PVA' – RC (PVA fibre) without mesh/grid, 'E-PVA-R' – FRC (PVA fibre) with mesh/grid, 'E-S' – FRC (steel fibre) without mesh/grid, 'E-S-R' – FRC (steel fibre) with mesh/grid,
'FM' is failure mode: 'F' – flexural failure, 'SH' – shear failure.
f'_c is cylinder compression strength. If the specimen uses cube compression strength, it shall be converted according to [62].
* Regarding ρ_f, it refers to the fibre reinforcement ratio of the textile in FRCM, and it refers to the volume fraction of fibre in mortar in ECC.

seem not to be effective even in the case of anchors and the failure mode observed is detachment. In cases where fully wrapped jackets were applied the failure mode changed from shear to flexural and fibre rupture was the observed mode of failure.

- The increase of FRCM reinforcement ratio, ρ_{cm}, leads to increased shear capacity for the strengthened beams, since the cross-sectional area (especially the width) of the RC beam is increased, thereby improving the shear capacity of the beam.
- In most of the FRC jacketed beams (74 %) no textiles (or grids) are used. The types of fibres used are PE, PVA, and steel up to 2 % fibre volume fraction.
- For the prediction of the shear strength contribution by the FRCM system, Triantafillou and Papanicolaou [51, Model 1], Escrig et al. [52, Model 2], and Tetta et al. [7, Model 3] models are based on fibre properties, whereas ACI [53, Model 4], Ombres [54, Model 5], and Younis et al. [37, Model 6] models are based on FRCM composite properties (effective strain and elastic modulus). The comparison of the average $V^{exp}_{FRCM}/V^{pred}_{FRCM}$ among the six models indicates that all the models except Triantafillou and Papanicolaou [51, Model 1] and Tetta et al. [7, Model 3] models underestimate the predicted shear strength provided by FRCM jacketing which is conservative. The models seem to perform less effectively for beams that failed by detachment. The dispersion of $V^{exp}_{FRCM}/V^{pred}_{FRCM}$ is the lowest for Triantafillou and Papanicolaou [51, Model 1] and Tetta et al. [7, Model 3] models.
- ACI 544 [55, Model 7], *fib* [56, Model 8], and Japan Society of Civil Engineers [61, Model 9] models were implemented to a limited number of FRC jacketed beams and based on the average values of $V^{exp}_{FRCM}/V^{pred}_{FRCM}$ the shear strength is underestimated. The dispersion of $V^{exp}_{FRCM}/V^{pred}_{FRCM}$ is very similar between the models. The data used are limited and further work is needed in the direction of generating experimental data and the development of reliable formulae.

The conclusions drawn from this review rely on the sampling presented in the compiled database in Appendix A. To verify the main observations made, future experimental studies, especially concerning FRC jacketing, are necessary to provide additional data. Several areas that require further investigation have been identified, including understanding the interaction between the internal shear reinforcement and the externally applied mortar-based composite jacket. Effective anchorage systems to prevent detachment of U-wrapped jacketed beams also need development. Defining the limiting effective strain of the fibre is crucial for improving existing models predicting the shear strength contribution of FRCM jackets. Moreover, there are gaps in existing studies on shear performance of RC beams strengthened with externally bonded mortar-based composites, necessitating more research and experimental testing on basalt-FRCM to validate its mechanical properties and potential in strengthening RC beams. A deeper understanding of the bond behaviour and load transfer mechanisms between internal shear reinforcement and the external jacket is essential for reliable design guidelines. Innovative anchorage solutions must be explored and evaluated to ensure the long-term durability and effectiveness of the strengthening system.

Moreover, existing predictive models for shear strength contribution of jackets lack accuracy, as they do not adequately consider critical factors such as the shear span-to-depth ratio and the mortar thickness. These factors have been observed to significantly influence the effectiveness of strengthening. Additionally, advancing the field of RC beam strengthening using FRCM composites requires a precise definition of the limiting effective strain of fibers. This parameter, which relates to the strain at which fiber detachment occurs, has a substantial impact on the overall performance of the FRCM jacket. Developing a reliable definition based on rupture strain or detachment failure strain of the textile reinforcement will enable the creation of more precise and reliable predictive models.

Declaration of Competing Interest

The authors declare that they have no known competing financial interests or personal relationships that could have appeared to influence the work reported in this paper.

Appendix A.

Table A1.

References

[1] Azam R, Soudki K. FRCM strengthening of shear-critical RC beams. J Compos Constr 2014;18(5):04014012.
[2] L.H. Sneed, J.A. Ramirez, Effect of depth on the shear strength of concrete beams without shear reinforcement–experimental study, 2008.
[3] Sherwood EG, Lubell AS, Bentz EC, Collins MP. One-way shear strength of thick slabs and wide beams. ACI Struct J 2006;103(6):794.
[4] Thermou G, Papanikolaou V, Lioupis C, Hajirasouliha I. Steel-Reinforced Grout (SRG) strengthening of shear-critical RC beams. Constr Build Mater 2019;216:68–83.
[5] Tetta ZC, Koutas LN, Bournas DA. Textile-reinforced mortar (TRM) versus fiber-reinforced polymers (FRP) in shear strengthening of concrete beams. Compos B Eng 2015;77:338–48.
[6] Gonzalez-Libreros JH, Sabau C, Sneed LH, Pellegrino C, Sas G. State of research on shear strengthening of RC beams with FRCM composites. Constr Build Mater 2017;149:444–58.
[7] Tetta ZC, Triantafillou TC, Bournas DA. On the design of shear-strengthened RC members through the use of textile reinforced mortar overlays. Compos B Eng 2018;147:178–96.
[8] Tetta ZC, Koutas LN, Bournas DA. Shear strengthening of full-scale RC T-beams using textile-reinforced mortar and textile-based anchors. Compos B Eng 2016;95:225–39.
[9] Azam R, Soudki K, West JS, Noël M. Behavior of shear-critical RC beams strengthened with CFRCM. J Compos Constr 2018;22(1):04017046.
[10] Marcinczak D, Trapko T, Musiał M. Shear strengthening of reinforced concrete beams with PBO-FRCM composites with anchorage. Compos B Eng 2019;158:149–61.
[11] Wakjira TG, Ebead U. Shear span-to-depth ratio effect on steel reinforced grout strengthened reinforced concrete beams. Eng Struct 2020;216:110737.
[12] Wakjira TG, Ebead U. Experimental and analytical study on strengthening of reinforced concrete T-beams in shear using steel reinforced grout (SRG). Compos B Eng 2019;177:107368.
[13] X. Yang, J.G. Dai, Z. Lu, Shear behavior of RC beams strengthened with FRP grid reinforced engineered cementitious composites, 6th Asia-Pacific Conference on FRP in Structures, APFIS 2017, 2017.
[14] Jongvivatsakul P, Bui LV, Koyekaewphring T, Kunawisarut A, Hemstapat N, Stitmannaithum B. Using steel fiber-reinforced concrete precast panels for strengthening in shear of beams: an experimental and analytical investigation. Advances in Civil Engineering 2019;2019.
[15] Garg V, Bansal PP, Sharma R. Retrofitting of Shear-Deficient RC Beams Using UHP-FRC, Iranian Journal of Science and Technology, Transactions of. Civ Eng 2019;43(3):419–28.
[16] Wang G, Yang C, Pan Y, Zhu F, Jin K, Li K, et al. Shear behaviors of RC beams externally strengthened with engineered cementitious composite layers. Materials 2019;12(13):2163.
[17] Hung C-C, Chen Y-S. Innovative ECC jacketing for retrofitting shear-deficient RC members. Constr Build Mater 2016;111:408–18.
[18] Wang B, Wang Z, Uji K, Zhang J, Guo R. Experimental investigation on shear behavior of RC beams strengthened by CFRP grids and PCM. Structures: Elsevier; 2020. p. 1994–2010.
[19] Thermou GE, Hajirasouliha I. Compressive behaviour of concrete columns confined with steel-reinforced grout jackets. Compos B Eng 2018;138:222–31.
[20] Wakjira TG, Ebead U. Internal transverse reinforcement configuration effect of EB/NSE-FRCM shear strengthening of RC deep beams. Compos B Eng 2019;166:758–72.
[21] Larbi AS, Contamine R, Ferrier E, Hamelin P. Shear strengthening of RC beams with textile reinforced concrete (TRC) plate. Constr Build Mater 2010;24(10):1928–36.
[22] Li VC. Tailoring ECC for special attributes: A review, International Journal of Concrete. Struct Mater 2012;6(3):135–44.
[23] Gonzalez-Libreros JH, Sneed L, D'Antino T, Pellegrino C. Behavior of RC beams strengthened in shear with FRP and FRCM composites. Eng Struct 2017;150:830–42.
[24] Wang G, Zhu F, Yang C. Experimental study on Shear behaviors of RC beams strengthened with ECC layers. In: IOP Conference Series: Materials Science and Engineering. IOP Publishing; 2020. p. 042024.
[25] Yang X, Gao W-Y, Dai J-G, Lu Z-D. Shear strengthening of RC beams with FRP grid-reinforced ECC matrix. Compos Struct 2020;241:112120.
[26] Attar HS, Esfahani MR, Ramezani A. Experimental investigation of flexural and shear strengthening of RC beams using fiber-reinforced self-consolidating concrete jackets. Structures: Elsevier; 2020. p. 46–53.
[27] Zhang HY, Yan J, Kodur V, Cao L. Mechanical behavior of concrete beams shear strengthened with textile reinforced geopolymer mortar. Eng Struct 2019;196:109348.
[28] Wei J, Wu C, Chen Y, Leung CK. Shear strengthening of reinforced concrete beams with high strength strain-hardening cementitious composites (HS-SHCC). Mater Struct 2020;53(4):1–15.
[29] Sakr MA, Sleemah AA, Khalifa TM, Mansour WN. Shear strengthening of reinforced concrete beams using prefabricated ultra-high performance fiber reinforced concrete plates: Experimental and numerical investigation. Struct Concr 2019;20(3):1137–53.
[30] Marcinczak D, Trapko T. The impact of the anchorage on the shear capacity of reinforced concrete beams. In: IOP Conference Series: Materials Science and Engineering. IOP Publishing; 2019. p. 012003.
[31] Marcinczak D, Trapko T. DIC (Digital Image Correlation) method in the research of RC beams strengthened with PBO-FRCM materials, E3S Web of Conferences. EDP Sciences 2019:03008.
[32] Tetta ZC, Koutas LN, Bournas DA. Shear strengthening of concrete members with TRM jackets: Effect of shear span-to-depth ratio, material and amount of external reinforcement. Compos B Eng 2018;137:184–201.
[33] Ebead U, Wakjira T. FRCM/stirrups interaction in RC beams strengthened in shear using NSE-FRCM, IOP Conference Series. Materials Science and Engineering, IOP Publishing 2018:112001.
[34] Younis A, Ebead U. Characterization and application of FRCM as a strengthening material for shear-critical RC beams, MATEC Web of Conferences. EDP Sciences 2018:09004.
[35] Azam R, Soudki K, West JS, Noël M. Shear strengthening of RC deep beams with cement-based composites. Eng Struct 2018;172:929–37.
[36] Sakr MA, Sleemah AA, Khalifa TM, Mansour WN. Behavior of RC beams strengthened in shear with ultra-high performance fiber reinforced concrete (UHPFRC). MATEC web of conferences: EDP Sciences; 2018. p. 09002.
[37] Younis A, Ebead U, Shrestha KC. Different FRCM systems for shear-strengthening of reinforced concrete beams. Constr Build Mater 2017;153:514–26.
[38] Aljazaeri ZR, Myers JJ. Strengthening of reinforced-concrete beams in shear with a fabric-reinforced cementitious matrix. J Compos Constr 2017;21(5):04017041.
[39] Awani O, El-Maaddawy T, El Refai A. Numerical simulation and experimental testing of concrete beams strengthened in shear with fabric-reinforced cementitious matrix. J Compos Constr 2016;20(6):04016056.
[40] Tetta ZC, Bournas DA. TRM vs FRP jacketing in shear strengthening of concrete members subjected to high temperatures. Compos B Eng 2016;106:190–205.
[41] Tzoura E, Triantafillou T. Shear strengthening of reinforced concrete T-beams under cyclic loading with TRM or FRP jackets. Mater Struct 2016;49(1):17–28.
[42] Ruano G, Isla F, Pedraza RI, Sfer D, Luccioni B. Shear retrofitting of reinforced concrete beams with steel fiber reinforced concrete. Constr Build Mater 2014;54:646–58.
[43] Kani G. The riddle of shear failure and its solution. Journal Proceedings 1964:441–68.
[44] Godat A, Hammad F, Chaallal O. State-of-the-art review of anchored FRP shear-strengthened RC beams: A study of influencing factors. Compos Struct 2020;254:112767.
[45] Chen J-F, Teng J. Shear capacity of FRP-strengthened RC beams: FRP debonding. Constr Build Mater 2003;17(1):27–41.
[46] Council NR. Guide for the design and construction of externally bonded FRP systems for strengthening existing structures, CNR-DT 200 R1. Rome: Italy; 2013. p. 1–143.
[47] Ary MI, Kang T-H-K. Shear-strengthening of reinforced & prestressed concrete beams using FRP: part I—review of previous research. International Journal of Concrete Structures and Materials 2012;6(1):41–7.
[48] Tanarslan HM, Yalçınkaya Ç, Alver N, Karademir C. Shear strengthening of RC beams with externally bonded UHPFRC laminates. Compos Struct 2021;262:113611.
[49] Eurocode C. 2: design of concrete structures–Part 1–1: general rules and rules for buildings: EN 1992-1-1. Brussels: CEN; 2004.
[50] Committee A. Building code requirements for structural concrete (ACI 318–08) and commentary. American Concrete Institute 2008.
[51] Triantafillou TC, Papanicolaou CG. Shear strengthening of reinforced concrete members with textile reinforced mortar (TRM) jackets. Mater Struct 2006;39(1):93–103.
[52] Escrig C, Gil L, Bernat-Maso E, Puigvert F. Experimental and analytical study of reinforced concrete beams shear strengthened with different types of textile-reinforced mortar. Constr Build Mater 2015;83:248–60.
[53] ACI, Guide to design and construction of externally bonded fabric-reinforced cementitious matrix (FRCM) systems for repair and strengthening concrete and masonry structures, Farmington Hills MI, USA, 2013.
[54] Ombres L. Structural performances of reinforced concrete beams strengthened in shear with a cement based fiber composite material. Compos Struct 2015;122:316–29.
[55] Aci. 544, Fiber Reinforced Concrete. American Concrete Institute 1997.
[56] *fib* Model Code, Design code for concrete structures, International Federation for Structural Concrete (fib) (2010).
[57] Guidelines for Concrete (9) 2006.
[58] Gowripalan N, Gilbert R. Design guidelines for ductal prestressed concrete beams. Reference Artical: The University of NSW; 2000.
[59] Bywalski C, Drzazga M, Kamiński M, Kaźmierowski M. A New Proposal for the Shear Strength Prediction of Beams Longitudinally Reinforced with Fiber-Reinforced Polymer Bars. Buildings 2020;10(5):86.

[60] Ali AMH. Shear strength and behavior of circular concrete members reinforced with FRP bars and spirals. Université de Sherbrooke 2016.
[61] Jsce. Standard specifications for concrete structures-2007, Design. Japan Society of Civil Engineers Tokyo (Japan) 2007.
[62] E.C. for Standardization, EN 1992-1-1 Eurocode 2: Design of concrete structures - Part 1-1: General ruels and rules for buildings, CEN, Brussels, 2005.